ผลของโพแทสเซียมและซีเรียมโปรโมเตอร์ต่อสมบัติของตัวเร่งปฏิกิริยานิกเกิลบนแกมมาอะลูมินา ในปฏิกิริยาคาร์บอนไดออกไซด์ไฮโดรจิเนชัน

นางสาวพิรุฬห์ลักษณ์ บุญวัฒน์

จุฬาลงกรณ์มหาวิทยาลัย
Chulalongkorn University

บทคัดย่อและแฟ้มข้อมูลฉบับเต็มของวิทยานิพนธ์ตั้งแต่ปีการศึกษา 2554 ที่ให้บริการในคลังปัญญาจุฬาฯ (CUIR)
เป็นแฟ้มข้อมูลของนิสิตเจ้าของวิทยานิพนธ์ ที่ส่งผ่านทางบัณฑิตวิทยาลัย
The abstract and full text of theses from the academic year 2011 in Chulalongkorn University Intellectual Repository (CUIR)
are the thesis authors' files submitted through the University Graduate School.

วิทยานิพนธ์นี้เป็นส่วนหนึ่งของการศึกษาตามหลักสูตรปริญญาวิศวกรรมศาสตรมหาบัณฑิต
สาขาวิชาวิศวกรรมเคมี ภาควิชาวิศวกรรมเคมี
คณะวิศวกรรมศาสตร์ จุฬาลงกรณ์มหาวิทยาลัย
ปีการศึกษา 2557
ลิขสิทธิ์ของจุฬาลงกรณ์มหาวิทยาลัย

THE EFFECT OF K AND Ce PROMOTERS ON THE PROPERTIES OF Ni/γ-Al_2O_3 CATALYSTS IN THE HYDROGENATION OF CO_2

Miss Phirunlak Boonyawat

A Thesis Submitted in Partial Fulfillment of the Requirements
for the Degree of Master of Engineering Program in Chemical Engineering
Department of Chemical Engineering
Faculty of Engineering
Chulalongkorn University
Academic Year 2014

Copyright of Chulalongkorn University

Thesis Title	THE EFFECT OF K AND Ce PROMOTERS ON THE PROPERTIES OF Ni/γ-Al_2O_3 CATALYSTS IN THE HYDROGENATION OF CO_2
By	Miss Phirunlak Boonyawat
Field of Study	Chemical Engineering
Thesis Advisor	Associate Professor Joongjai Panpranot, Ph.D.

Accepted by the Faculty of Engineering, Chulalongkorn University in Partial Fulfillment of the Requirements for the Master's Degree

.....Dean of the Faculty of Engineering

(Professor Bundhit Eua-arporn, Ph.D.)

THESIS COMMITTEE

.....Chairman

(Associate Professor Bunjerd Jongsomjit, Ph.D.)

.....Thesis Advisor

(Associate Professor Joongjai Panpranot, Ph.D.)

.....Examiner

(Chutimon Satirapipathkul, D.Eng.)

.....External Examiner

(Assistant Professor Okorn Mekasuwandumrong, D.Eng.)

พิรุฬห์ลักษณ์ บุญวัฒน์ : ผลของโพแทสเซียมและซีเรียมโปรโมเตอร์ต่อสมบัติของตัวเร่งปฏิกิริยานิกเกิลบนแกมมาอะลูมินาในปฏิกิริยาคาร์บอนไดออกไซด์ไฮโดรจิเนชัน (THE EFFECT OF K AND Ce PROMOTERS ON THE PROPERTIES OF Ni/γ-Al_2O_3 CATALYSTS IN THE HYDROGENATION OF CO_2) อ.ที่ปรึกษาวิทยานิพนธ์หลัก: รศ. ดร. จูงใจ ปั้นประณต, 87 หน้า.

งานวิจัยนี้ศึกษาผลของโปรโมเตอร์ (ซีเรียม, โพแทสเซียม แลนทานัม, แมงกานีส และแมกนีเซียม) ต่อสมบัติของตัวเร่งปฏิกิริยานิกเกิลบนอะลูมินาที่เตรียมโดยวิธีการเคลือบฝังแบบเปียกในปฏิกิริยาไฮโดรจิเนชันของคาร์บอนไดออกไซด์ที่อุณหภูมิ 500 องศาเซลเซียส ความดันบรรยากาศ ตัวเร่งปฏิกิริยาที่เติมโปรโมเตอร์ให้ค่าร้อยละการเปลี่ยนของคาร์บอนไดออกไซด์สูงขึ้น เนื่องมาจากความสามารถในการรีดักชันสูงขึ้นและปริมาณโลหะที่ว่องไวต่อการทำปฏิกิริยาเพิ่มสูงขึ้น โดยตัวเร่งปฏิกิริยาทุกตัวให้ค่าการเลือกเกิดของมีเทนเกือบ100% จากนั้นศึกษาผลของวิธีการเตรียมตัวเร่งปฏิกิริยาบนตัวเร่งปฏิกิริยานิกเกิลบนอะลูมินาที่โปรโมทด้วยซีเรียมและโพแทสเซียมโดยเปรียบเทียบระหว่างวิธีการทำปฏิกิริยาในภาวะของแข็งและวิธีการเตรียมแบบเคลือบฝัง พบว่าตัวเร่งปฏิกิริยานิกเกิลบนอะลูมินาที่เตรียมโดยวิธีเคลือบฝังที่โปรโมทด้วยโพแทสเซียมมีประสิทธิภาพสูงสุดในการทำปฏิกิริยาโดยให้ค่าร้อยละการเปลี่ยนของคาร์บอนไดออกไซด์เป็น 82.03 สำหรับตัวเร่งนิกเกิลบนอะลูมินาที่ไม่ได้ปรับปรุงตัวเร่งปฏิกิริยาที่เตรียมโดยวิธีการเคลือบฝังให้ค่าร้อยละการเปลี่ยนของคาร์บอนไดออกไซด์ในการทำปฏิกิริยาสูงกว่าการเตรียมด้วยวิธีปฏิกิริยาในภาวะของแข็ง แต่เมื่อนำเครื่องบดแบบลูกบอลมาช่วยในการเตรียมตัวเร่งด้วยวิธีการทำปฏิกิริยาในภาวะของแข็งค่าร้อยละการเปลี่ยนของคาร์บอนไดออกไซด์มีค่าสูงขึ้น ความแตกต่างที่พบระหว่างการเตรียมทั้งสองวิธีคือขนาดอนุภาคและบริเวณที่อยู่ของนิกเกิลบนพื้นผิวตัวรองรับอะลูมินา ผลการวิเคราะห์ด้วยเทคนิคเอ็กซ์เรย์โฟโตอิเล็กตรอนสเปกโตรสโกปีแสดงอนุภาคนิกเกิลออกไซด์บนพื้นผิวด้านนอกของตัวรองรับอะลูมินาที่เตรียมด้วยวิธีการทำปฏิกิริยาในภาวะของแข็ง อย่างไรก็ตามตัวเร่งปฏิกิริยาที่เตรียมโดยวิธีการทำปฏิกิริยาในภาวะของแข็งให้ประสิทธิภาพดีที่สุดเมื่อใช้เครื่องบดแบบลูกบอลและปรับปรุงด้วยซีเรียม โดยให้ค่าร้อยละการเปลี่ยนแปลงของคาร์บอนไดออกไซด์เป็น 81.16 ซึ่งเทียบได้กับตัวเร่งนิกเกิลบนอะลูมินาที่ปรับปรุงด้วยโพแทสเซียมเตรียมโดยการเคลือบฝัง ทั้งนี้ประสิทธิภาพของตัวเร่งปฏิกิริยามีความสัมพันธ์สอดคล้องกับค่าการกระจายตัวของนิกเกิลและปริมาณของนิกเกิลที่ว่องไวในการทำปฏิกิริยา

ภาควิชา วิศวกรรมเคมี ลายมือชื่อนิสิต .....

สาขาวิชา วิศวกรรมเคมี ลายมือชื่อ อ.ที่ปรึกษาหลัก .....

ปีการศึกษา 2557

5670318021 : MAJOR CHEMICAL ENGINEERING
KEYWORDS: PROMOTER / CARBON DIOXIDE HYDROGENATION / NICKEL CATALYST / SOLID-STATE REACTION

PHIRUNLAK BOONYAWAT: THE EFFECT OF K AND Ce PROMOTERS ON THE PROPERTIES OF Ni/γ-Al_2O_3 CATALYSTS IN THE HYDROGENATION OF CO_2. ADVISOR: ASSOC. PROF. JOONGJAI PANPRANOT, Ph.D., 87 pp.

The effect of promoters (Ce, K, La, Mg, and Mn) on the catalytic properties of Ni/Al_2O_3 catalysts prepared by incipient wetness impregnation method (imp) were investigated in carbon dioxide hydrogenation at 500 °C and 1 atm. All the promoted Ni/Al_2O_3 catalysts exhibited in higher CO_2 conversion than the non-promoted ones, which may be attributed to their higher reducibility and higher number of active Ni species. All the Ni-based catalysts showed CH_4 selectivity nearly 100%. The effect of preparation method was further investigated on K and Ce promoted Ni/Al_2O_3 catalysts by comparing the solid-state reaction method (ss) with and without dry ball milling and the imp method. The imp_Ni-K/Al_2O_3 was found to be the most efficient catalyst giving the highest CO_2 conversion at 82.03%. According to the CO chemisorption results, the amounts of nickel active sites of the non-promoted ss_Ni/Al_2O_3 catalysts were lower than the ones prepared by impregnation but when dry ball milling was applied in the preparation of Ni/Al_2O_3 catalysts by ss method, the CO_2 conversion increased. The main differences in the characteristics of the catalysts prepared by solid-state reaction and impregnation were probably the Ni particle sizes and the location of Ni particles on the support. The XPS results suggest that nickel oxide particles were deposited on the external surface of the alumina supports when prepared by the ss method. The best performance among the ss catalysts was obtained over the bm_Ni-Ce/Al_2O_3 with CO_2 conversion as 81.16%, which were comparable to the imp_Ni-K/Al_2O_3. The catalysts performances were correlated well with high Ni %dispersion and the amount of Ni active sites.

Department: Chemical Engineering Student's Signature .....
Field of Study: Chemical Engineering Advisor's Signature .....
Academic Year: 2014

ACKNOWLEDGEMENTS

The author would like to express her appreciation and gratefulness to her advisor, Associate Professor Joongjai Panpranot for her suggestion, knowledge and the best guidance in this study. Especially her support and encouragement which are invaluable.

In addition, I would also like to thank to Associate Professor Bunjerd Jongsomjit, the chairman of the committee for this thesis, and Chutimon Satirapipathkul, D.Eng., Assistant Professor Okorn Mekasuwandamrong, D.Eng., members of this thesis committee for their kind assistance.

Most of all, the author would like to thank her parents for all their support who always back up and give their suggestion for each problem. This achievement is to be the present for her parents.

Moreover, I would like to thank, Assistant Professor Thanakorn Wasanapiarnpong, D.Eng., his suggestion and his department from Department of Materials, Faculty of Science, Chulalongkorn University for two roll mill machine and all equipment supports.

Furthermore, the author would like to thank all her friends, members of the Center of Excellent on Catalysis & Catalytic Reaction Engineering, Department of Chemical Engineering, Chulalongkorn University for their advices, support, motivation and nice friendship. I would like to thank you sincerely.

Lastly, the author would be grateful the department of Chemical Engineering and Chulalongkorn University for their supports.

จุฬาลงกรณ์มหาวิทยาลัย
Chulalongkorn University

CONTENTS

Page

THAI ABSTRACT iv

ENGLISH ABSTRACT v

ACKNOWLEDGEMENTS vi

CONTENTS vii

LIST OF TABLE xi

LIST OF FIGURE xiii

CHAPTER I INTRODUCTION 1

1.1 Introduction 1

1.2 Objectives 3

1.3 Research scopes 4

1.4 Benefits 4

1.5 Research Methodology 5

CHAPTER II THEORY AND LITERATURE REVIEWS 7

2.1 Carbon dioxide hydrogenation reaction 7

2.2 Milling /Grinding 9

2.2.1 Ball Mill 10

2.2.1.2 Types of milling media balls. 11

2.3 solid state reaction 14

2.4 Active element for methanation reaction, CO hydrogenation and CO_2 hydrogenation 17

2.4.1 Metal-base catalysts 17

2.4.2 Nickel 19

2.5 Alumina 22

จุฬาลงกรณ์มหาวิทยาลัย
CHULALONGKORN UNIVERSITY

Page

CHAPTER III EXPERIMENTAL 29
3.1 Chemicals 29
3.2 Materials preparation 29
3.2.1 Catalyst preparation by incipient wetness impregnation 29
3.2.2 Catalyst preparation by solid state reaction 30
3.3 Catalysts characterization 30
3.3.1 X-ray diffraction (XRD) 30
3.3.2 N_2 physisorption 30
3.3.3 Scanning electron microscopy (SEM) 31
3.3.4 X-ray photoelectron spectroscopy (XPS) 31
3.3.5 Temperature-programmed reduction (TPR) 31
3.3.6 Carbon mono oxide chemisorption 31
3.3.7 Particle size analysis 32
3.4 Reaction in carbon dioxide hydrogenation 32
3.4.1 Materials 32
3.4.2 Apparatus 32
3.4.2.1 Reactor 33
3.4.2.2 Electrical furnace 33
3.4.2.3 Temperature controller 33
3.4.2.4 Gas controlling system 33
3.4.2.5 Gas chromatography 33
3.4.3 The CO_2 hydrogenation procedures 33
CHAPTER IV RESULTS AND DISCUSSION 35

Chulalongkorn University

Page

4.1 Effect of promoter (K, Mn, La, Ce, and Mg) on the Ni/Al_2O_3 catalysts prepared by impregnation 35

4.1.1 Catalysts characterization 36

4.1.1.1 X-ray diffraction (XRD) 36

4.1.1.2 Nitrogen physisorption 38

4.1.1.3 Hydrogen temperature program reduction (H_2-TPR) 39

4.1.1.4 Scanning electron microscopy analyses (SEM) 41

4.1.1.5 Carbon monoxide chemisorption 42

4.1.2 The catalytic performance of the Ni/Al_2O_3 catalysts in carbon dioxide hydrogenation. 44

4.2 Effect of K and Ce promoters on the Ni/Al_2O_3 catalysts prepared by solid-state reaction with and without dry ball mill and compare to the conventional impregnation method. 46

4.2.1 Catalysts characterization 47

4.2.1.1 X-ray diffraction (XRD) 47

4.1.1.2 Nitrogen physisorption 49

4.2.1.3 Hydrogen temperature program reduction (H_2-TPR) 51

4.2.1.4 Scanning electron microscopy analyses (SEM) 54

4.2.1.5 Carbon mono oxide chemisorption 56

4.2.1.6 X-ray photoelectron spectroscopy (XPS) 57

4.2.1.6 Particle size analysis 59

4.2.2 The catalytic performance of the Ni/Al_2O_3 catalysts in carbon dioxide hydrogenation 61

CHAPTER V CONCLUSIONS AND RECOMMENDATIONS 66

จุฬาลงกรณ์มหาวิทยาลัย
Chulalongkorn University

Page

5.1 Conclusions 66

5.2 Recommendations 67

REFERENCES 68

APPENDIX A 75

APPENDIX B 80

APPENDIX C 83

APPENDIX D 84

VITA 87

จุฬาลงกรณ์มหาวิทยาลัย
Chulalongkorn University

LIST OF TABLE

Page

Table 2.1 Characteristics of different types of balls. 12

Table 2.2 The formation of homogeneous solid phase 15

Table 2.3 Advantage and disadvantage of solid state reaction 17

Table 2.4 Information of nickel 20

Table 2.5 Summary of Literature reviews catalysts in methanation reaction, CO hydrogenation and CO_2 hydrogenation 26

Table 3.1 Chemicals used for synthesis of the catalysts 29

Table 3.2 Gas materials are used to catalytic activity test. 32

Table 3.3 The operating conditions for GC 34

Table 4.1 Average NiO crystallite size of Ni-based catalysts with different promoters 37

Table 4.2 Physiochemical of Ni-based catalysts prepared by impregnation methods 38

Table 4.3 H_2 consumption of non-promoted and promoted nickel catalysts 41

Table 4.4 CO chemisorption of non-promoted and promoted nickel catalysts 43

Table 4.5 The CO_2 conversion and product selectivity during CO_2 hydrogenation of nickel catalyst 45

Table 4.6 Average NiO crystallite size of Ni-based catalysts with Ce, K promoters prepared by the solid-state reaction with and without dry ball including the incipient wetness impregnation 49

Table 4.7 Physiochemical of Ni-based catalysts with Ce, K promoters prepared by the solid-state reaction with and without dry ball including the incipient wetness impregnation 50

จุฬาลงกรณ์มหาวิทยาลัย
Chulalongkorn University

Page

Table 4.8 H_2 consumption of Ni-based catalysts with Ce, K promoters prepared by the solid-state reaction and the incipient wetness impregnation..... 52

Table 4.9 CO chemisorption of Ni-based catalysts with Ce, K promoters prepared by the solid-state reaction with and without dry ball including the incipient wetness impregnation..... 57

Table 4.10 The binding energy, FWHM of Ni $2p_{3/2}$ and the ratio of percentages of atomic concentration of the nickel catalysts..... 58

Table 4.11 Particle size of of Ni-based catalysts with Ce, K promoters prepared by the solid-state reaction with and without dry ball including the incipient wetness impregnation..... 60

Table 4.12 The conversion and product selectivity during CO_2 hydrogenation of nickel catalysts..... 63

Table D.1 Condition use in Shimadzu modal GC-8A..... 86

จุฬาลงกรณ์มหาวิทยาลัย
Chulalongkorn University

LIST OF FIGURE

Page

Figure 1.1 Sequence of dehydration and transformation of alumina from gibbsite and bochmite 3

Figure 1.2 Flow diagram of research methodology of part 1 5

Figure 1.3 Flow diagram of research methodology of part 2 6

Figure 2.1 Catalytic routes for carbon dioxide activation in heterogeneous phase [26]. 7

Figure 2.2 The pathways of carbon dioxide methanation on supported metal catalysts 8

Figure 2.3 Ball milling terminology 11

Figure 2.4 Decomposition sequences of aluminum hydroxides [9]. 23

Figure 4.1 The XRD patterns of support and Ni/Al_2O_3 catalysts with different promoters 36

Figure 4.2 The TPR profiles of Ni/Al_2O_3 catalysts with different promoter 39

Figure 4.3 The SEM images of Ni/Al_2O_3 catalysts with different type promoters: a) imp_Ni/Al_2O_3, b) imp_Ni-Ce/Al_2O_3, c) imp_Ni-K/Al_2O_3, d) imp_Ni-La/Al_2O_3, e) imp_Ni-Mn/Al_2O_3 and f) imp_Ni-Mg/Al_2O_3. 42

Figure 4.4 The catalytic activities of the Ni/Al_2O_3 catalysts in CO_2 hydrogenation. 45

Figure 4.5 The XRD patterns of support and Ni/Al_2O_3 catalysts with Ce, K promoters prepared by the solid-state reaction with and without dry ball including the incipient wetness impregnation 47

Figure 4.6 The TPR profiles of Ni/Al_2O_3 catalysts with Ce, K promoter prepared by a.) impregnation, b.) solid-state reaction without dry ball mill and c.) solid-state reaction with dry ball mill 53

Page

Figure 4.7 The SEM images of $Ni/A_{l2}O_3$ catalysts with Ce, K promoter prepared by impregnation, solid-state reaction without dry ball mill and solid-state with dry ball mill. 55

Figure 4.8 XPS energy spectrum for Ni 2p levels in of the sample of nickel catalysts. 59

Figure 4.9 The catalytic activities in carbon dioxide hydrogenation of Ni/Al_2O_3 catalysts with Ce, K promoter prepared a.) impregnation, b.) solid-state reaction without dry ball mill and c.) solid-state reaction with dry ball mill..... 64

Figure 4.10 The catalytic activities in carbon dioxide hydrogenation of non-promoted Ni/Al_2O_3 catalysts prepared by the solid-state reaction with and without dry ball mill and the incipient wetness impregnation 65

Figure B.1 The measured peak of imp_Ni-K/Al_2O_3 to calculate the crystallite size 82

Figure B.2 The plot indicating the value of line broadening due to the equipment that was obtained by using α-alumina as standard. 82

Figure D.1 The calibration curve of carbon dioxide 84

Figure D.2 The calibration curve of carbon monoxide 85

Figure D.3 The calibration curve of methane 85

จุฬาลงกรณ์มหาวิทยาลัย
Chulalongkorn University

CHAPTER I
INTRODUCTION

1.1 Introduction

Recently, oil and natural gas resources have more demand, however they become scarce and their prices continue to rise [1-3]. Therefore, The production and the development of alternative energies can be a good choice for solving the problem of limited energy which scientists and engineer in this field give much of their interests on [4]. Carbon dioxide hydrogenation is one choice which can produce synthetic fuels.

Carbon dioxide hydrogenation (1) has two step-reactions. The First step reaction is reverse water-gas shift (2) and the second step reaction is CO hydrogenation (3)

$$CO_2\ (g) + 4H_2\ (g) \rightarrow CH_4\ (g) + 2H_2O\ (g) \quad (1)$$

$$CO_2\ (g) + H_2\ (g) \rightarrow CO\ (g) + H_2O\ (g) \quad (2)$$

$$CO\ (g) + 3H_2\ (g) \rightarrow CH_4\ (g) + H_2O\ (g) \quad (3)$$

Carbon dioxide hydrogenation reaction is an environmental friendliness method that helps to reduce the amount of CO_2 emission by releasing it in high amount from natural and human's activity which takes up the highest portion among greenhouse gas. Therefore, CO_2 is one of the main factors which lead to global warming [5-7]. It is a good idea to add value to the CO_2 instead of just letting it flow in the air. This reaction changes carbon dioxide into methane (CH_4) that is the main product. This makes CO_2 hydrogenation becomes an alternative source of natural gas (>95% methane, high HHV) [8-10].

Normally, several metal-based catalysts are used in catalytic hydrogenation reaction. Such as, Ni [1, 2, 4, 8, 9, 11-13], Fe [14], Ru [13, 14], Co [13, 15-17] and Pt [13] supported on several oxide supports including SiO_2 [18] , TiO_2 [19] and Al_2O_3 [1, 2, 4, 8, 9, 11]. One of the most attracting metals, according to its high activity and selectivity for methane formation, is Ni-based catalyst. The price of Ni-based catalysts

is affordable compared to noble metals, so it suits for industrial applications [2, 8, 11]. Alumina (Al_2O_3) is a common material used as coating, catalysts, catalyst supports, sorbent and ceramics [20]. Alumina is one of supports which are frequently used for preparing nickel catalysts. However, there is several transition phases of alumina such as gamma (γ) alumina, eta (η), kappa (κ), chi (χ)and delta (δ) [21]. In Figure 1.1, the phase transformation of alumina is demonstrated by beginning from gibbsite ($Al(OH)_3$). Heating rate, temperature, pressure, and initial raw material are the factors which lead to the phrase transformation of Alumina. Nowadays, γ-Al_2O_3 is the most popular structure used as a support for metal catalyst. Moreover, it has several applications because of its thermal properties, characteristic mechanical, chemical, and high surface area compared to the other oxides [22].

Nickel catalysts supported on alumina are essential catalyst systems widely used in several reactions such as hydrogenation, hydro-treating, and stream reforming. However, engineers and researchers in this field still see the needs of the development in the performance of Ni catalysts, especially in terms of its activity, selectivity and stability. The addition of a second metal promoter can improve the nickel-based catalyst properties in carbon dioxide hydrogenation [23, 24]. For example, Znak et al. (2005) reported that the effect of Ce, La, and Zr on Ni/Al_2O_3 in CO and CO_2 hydrogenation. The catalysts was prepared by a co-impregnation method of NiO/Al_2O_3 with aqueous solutions $La(NO_3)_3$, $Ce(NO_3)_3$, and $Zr(NO_3)_2$. The result shows cerium, lanthanum and zirconium promoted dissociation of CO which led to the increasing catalytic activity of NiO/Al_2O_3 catalysts. The impregnation method is considered as the preparation method which is the most extensive for catalyst. However, steps such as drying and calcination are necessary. The solid-state reaction is the mixture of materials that is the direct reaction. The benefits of this method are the simpler, cheaper, and higher yields of products [25]. Ball mill, a machine generally used in industrial and laboratory, help to prepare the catalysts by solid state reaction. Moreover, this makes the process easier to scale up, convenient operation, absence wastes and presenting minimal environmental. The process parameters considered for using ball mill such as milling time and rotation speed.

In this research, the aim is to study the effect of promoters on the performances of Ni/Al_2O_3 in the CO_2 Hydrogenation. The preparations by solid-state reaction, with and without dry ball mill were compared to the conventional impregnation method. All the catalysts were investigated in the carbon dioxide hydrogenation. The catalysts were characterized by X-ray diffraction (XRD), hydrogen temperature program reduction (H_2-TPR), and N_2 physisorption, scanning electron microscope analyses (SEM), X-ray photoelectron spectroscopy (XPS) and CO chemisorption, Particle size analysis. The catalytic performances of Ni/Al_2O_3 catalysts were studied in the carbon dioxide hydrogenation at 500°C and atmospheric pressure.

Figure 1.1 Sequence of dehydration and transformation of alumina from gibbsite and bochmite

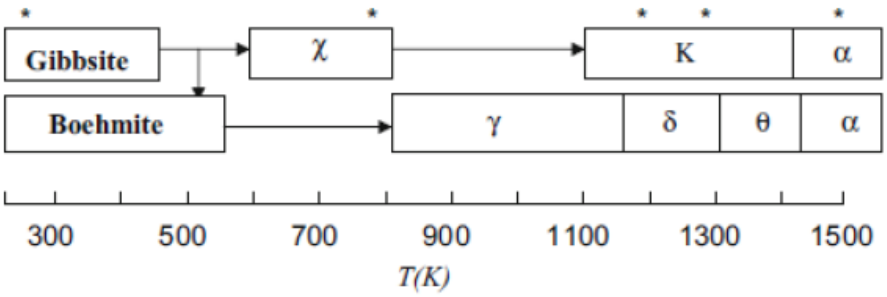

1.2 Objectives

The objectives of this research are divided in to two parts.

Past1: To study the effect of potassium, manganese, lanthanum, cerium and magnesium on the properties of nickel/alumina catalysts prepared by impregnation method in CO_2 hydrogenation.

Past2: To prepare the Ni/γ-Al_2O_3 catalysts with selected promoters by solid-state reaction with and without dry ball milling and investigated their properties in CO_2 hydrogenation.

1.3 Research scopes

1.3.1 Study of the relating research

1.3.2 Preparation of Ni/γ-Al_2O_3 catalysts with different promoters (K, Mn, La, Ce, and Mg) by incipient wetness impregnation, using calcination at 500°C.

1.3.3 Preparation Ni-based catalysts with selected promoters by solid-state reaction using the mixture of nickel nitrate, gibbsite, and different promoters at 500°C with and without dry ball milling.

1.3.4 Catalytic performance test for the carbon dioxide hydrogenation of Ni/Al_2O_3 catalysts using 8.8% CO_2 in H_2 as feeding-reactants at reaction temperature 500°C and 1 atm total pressure in a quartz fixed-bed reactor.

1.3.5 Characterization of Ni/γ-Al_2O_3 catalysts with different promoters using X-ray diffraction (XRD), Scanning electron microscope (SEM), Nitrogen physisorption, Hydrogen temperature program reduction (H_2-TPR), CO chemisorption, Particle size analysis and X-ray photoelectron spectroscopy (XPS).

จุฬาลงกรณ์มหาวิทยาลัย
Chulalongkorn University

1.4 Benefits

1.4.1 To obtain suitable promoter for preparation of Ni/γ-Al_2O_3 catalyst for CO_2 hydrogenation.

1.4.2 To obtain suitable method for preparation of Ni/γ-Al_2O_3 catalysts for CO_2 hydrogenation.

1.4.3 The results of this research will be used as information for industrial process.

1.5 Research Methodology

1.5.1 **Part 1**: Study of effect in promoted Ni/γ-Al_2O_3 catalysts with K, Mn, La, Ce and Mg by incipient wetness impregnation.

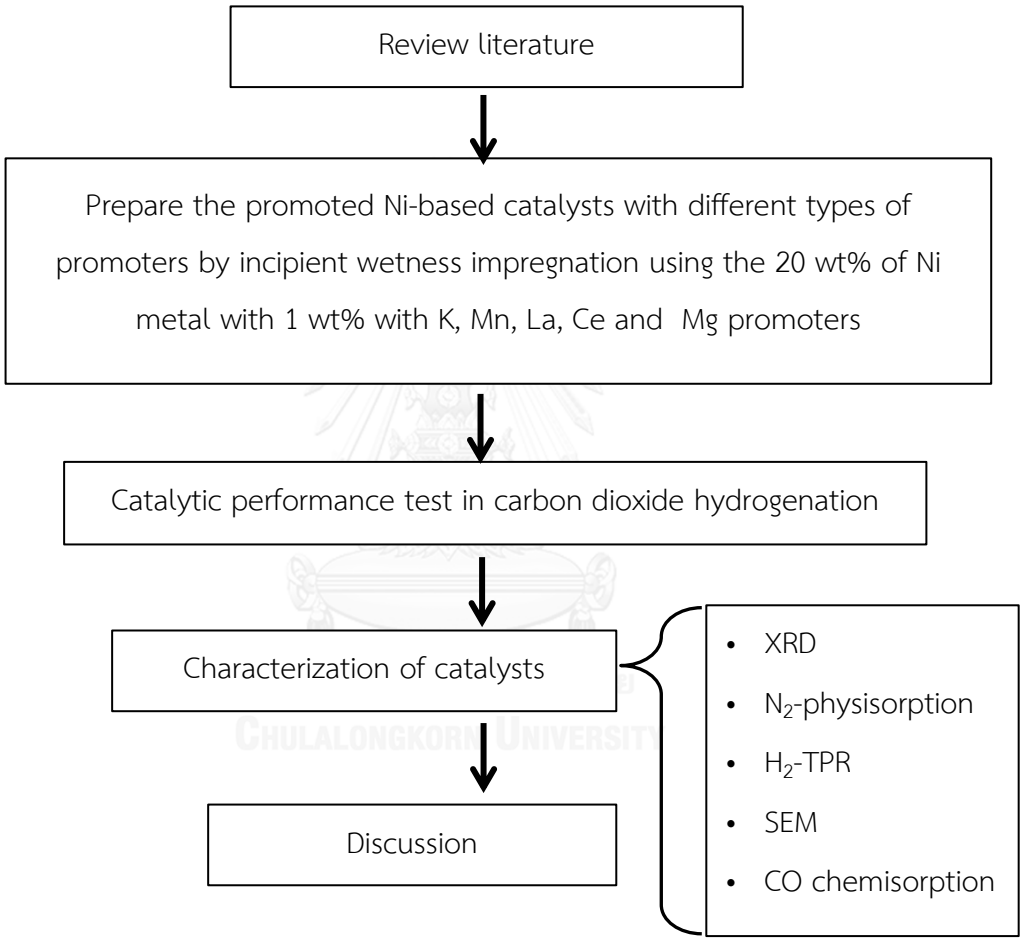

Figure 1.2 Flow diagram of research methodology of part 1

1.5.2 **Part 2:** Study of effect in selected promoter on Ni/γ-Al_2O_3 catalysts by solid-state reaction, with and without dry ball mill, and compare to the conventional impregnation method.

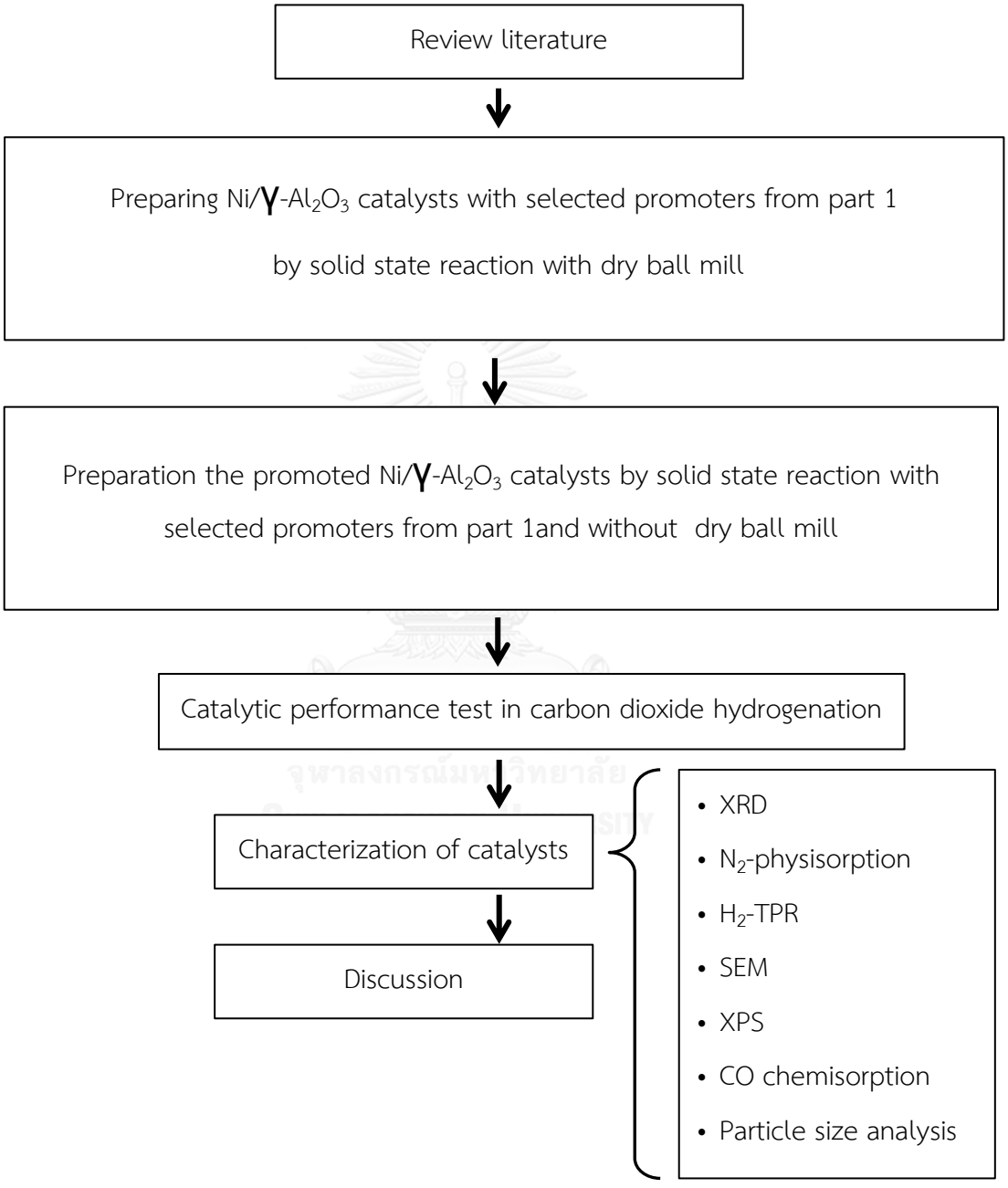

Figure 1.3 Flow diagram of research methodology of part 2

CHAPTER II

THEORY AND LITERATURE REVIEWS

2.1 Carbon dioxide hydrogenation reaction

Nowadays, there is the realization that supplies of fuels such as oil and natural gas are rare. As a result there has been an increasing attentions focus on the conversion of fuels from a less to a more desirable form. CH_4 synthetic gas is an alternative energy produced from CO_2 hydrogenation. This reaction is an environmentally friendliness reaction because it reduces CO_2 released in the air, led to global warming [1, 11, 15, 17]. Therefore, people want to change the CO_2 by adding its value. For example methanol, renewable fuels, Organic carbonate with catalytic process shown in Figure 2.1

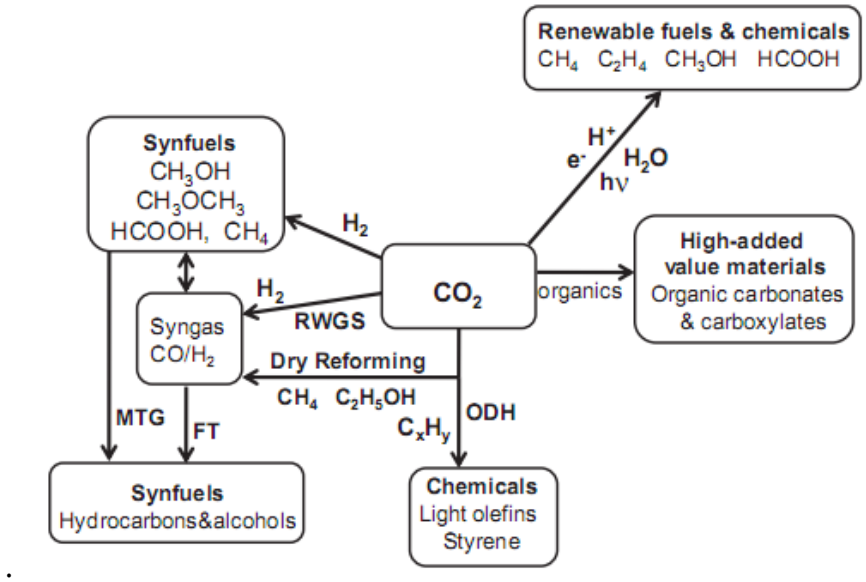

Figure 2.1 Catalytic routes for carbon dioxide activation in heterogeneous phase [26].

Carbon dioxide hydrogenation (1) is an exothermic reaction with ΔH_{298K} = -252.9 kJ/mole that has two step-reactions : reverse water gas shift (2) and CO hydrogenation (3)

CO_2 (g) +4H_2 (g) → CH_4 (g) + 2H_2O (g); ΔH_{298K} = -252.9 kJ/mole (1)

CO_2 (g) + H_2 (g) → CO (g) + H_2O (g) (2)

CO (g) + 3H_2 (g) → CH_4 (g) + H_2O (g) (3)

The synthesis of CO_2 methanation has two main mechanisms Shown in Figure 2.2

First mechanisms; the CO_2 and H_2 gas was changed to CO form. After that, it converses to methane. The adsorbed formyl species $(HCO)_{ads}$ or surface carbon (C_{ads}) are the intermediates that can be hydrogenated to produce methane.

Second mechanisms; CO_2 is directly hydrogenated that doesn't occur in intermediate CO formation. It could be that the hydrogen carbonate $(HCO_3)_{ads}$ and formate $(HCOO)_{ads}$ species are intermediates. The key step of the methane formation is intermediates adsorbed on the metal-support interface.

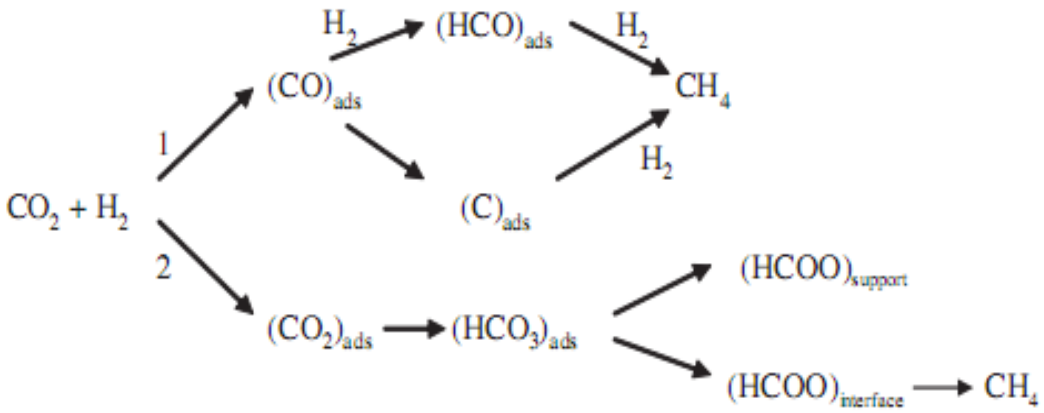

Figure 2.2 The pathways of carbon dioxide methanation on supported metal catalysts [26].

CO_2 hydrogenation reaction which occurs could be undesired. Such as reactions producing carbon that can deposit on the catalyst to cause loss of activity.

$$2CO \rightleftarrows CO_2 + C$$
$$CO + H_2 \rightleftarrows H_2O + C$$
$$CH_4 \rightleftarrows 2H_2 + C$$

According to previous researches and studies, thermodynamics designers can conclude that high conversion to methane could attain at the order of 25 atm pressure. Carbon deposition would be favored in high temperature and low pressure, if the hydrogen:carbon monoxide ratio was less than 2.5. Moreover, the thermodynamic is very exothermic reaction, and that carbon formation would be favored at higher temperatures (see above). So, Methanation would not be favored at above 620°C [27].

2.2 Milling /Grinding

The milling of materials has been essential unit operation in many industrial sectors such as the mineral, chemical, ceramic processing, metallurgy, pharmaceutical, food and powder metallurgy industries. The purposes of mechanical milling are particle size reduction, mixing or blending, particle shape changes and synthesis of nano-composite [28]. Recently, there are emphasizes of the importance of milling in powder due to the increasing usage of powders. Compare to other methods, ball milling has the advantages because it is a cheap method, has a simple process, has small environmental problems, easier to scale up, convenient operation and absence of wastes.

For example, group of equipment and the principles of grinding (milling) as follows[29]:

I. **Ball Mill** is a grinding process based on the method of cylinder rotation which has the ball inside. It can be divided into Batch mill and Continuous Mill. These two types of milling can grind materials in both wet and dry milling.

II. **Attrition Mill** is to grind the material to resolution and low distribution particle sizes. The particle's size is less than 1 μm (Depending on the size of precursor, hardness of materials, type and amount of ball and milling time)

III. **Jet Mill** is a grinding process without ball mill. But it's raw materials move in a very high speed to grind themselves.

IV. **Vibro Mill or Vibration Mill** is a machine which relies on a vibrating rod mill and materials to grind themselves.

V. **Pendula Mill** is a machine to grind only dry materials. The hammer hits and us e the wind to divide the size of particle.

The choice is determined by the end results required, and the chemical and physical of the powder.

จุฬาลงกรณ์มหาวิทยาลัย
Chulalongkorn University

2.2.1 Ball Mill

Ball Mill is used to reduce particle sizes or mix particles that have simple accessories that show in Figure 2.3. It can be divided into Batch mill and Continuous mill which can grind both dry and wet materials. For dry milling, normally use grinding and mixing material such as Limestone, Feldspar and SiO_2.

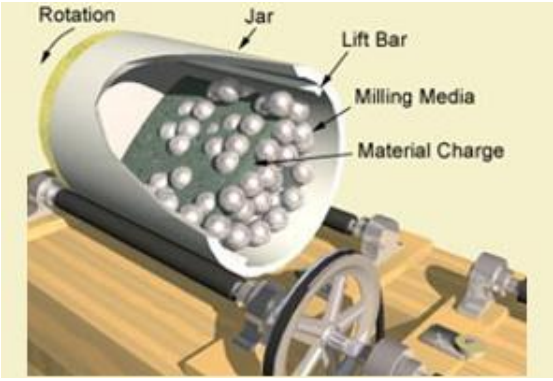

Figure 2.3 Ball milling terminology

2.2.1.1 Factors which make the good quality from grinding

1. The amount of milling media balls used in rotating Cylinder jar.

2. The size of milling media ball and portion of each different size of balls

3. Type of milling media ball

4. Type of cylinder jar

5. Rotating speed (Critical Speed)

6. The amount of milling media balls in Batch Mill

จุฬาลงกรณ์มหาวิทยาลัย
Chulalongkorn University

In order to get the most efficient quality from grinding, adding 50-55% of milling media balls in rotating cylinder jar of its total volume. The study found that by using this amount of balls will take up the least milling time. Also, the value of particle size distribution is the best.

2.2.1.2 Types of milling media balls.

Balls with high density such as Alumina balls increase the efficient of grinding and reduce milling time. The example of balls and information are shown in the table 2.1 below.

Table 2.1 Characteristics of different types of balls.

Name	Composition	Specific gravity	Performance in grinding	Price	% Wear
Flint	SiO_2	2.5 to 2.6	Moderate to low	Cheap	High
Porcelain	Al_2O3, SiO_2	2.3 to 2.6	Moderate	Moderate	High
Steatite	SiO_2, MgO, Al_2O_3	2.6 - 2.8	Moderate	Moderate	Moderate
Alumina	Al_2O_3	3.5 to 3.7	High	High	Little
Zirconia	ZrO_2	5.8 to 6.0	Very high	Very high	Low

In many researches, milling and grinding have been generally used in the studies to prepare materials, as well as, in the research about catalytic reaction. Ball mill can also be used to prepare the catalysts with many purposes, such as, in particles sizes reduction and physical mixing.

Kumar et al. (2012) investigated the effect of ball milling on alumina mixed nickel, magnetite and Raney nickel in reaction between NaOH and CO. This leads to the formation of Na_2CO_3 and H_2 .The catalysts were determined to get the optimum particle size for the catalysts. Raney nickel with average crystallite size of 209 Å that preparation of 2 h with ball mill shows the best performance because Raney nickel has the best effect for NaOH-CO reaction. Particle size of the catalysts has an effect on the reaction yield. For alumina mixed with nickel or Raney nickel catalysts was decrease in the catalytic activity when use longer time milling. However, magnetite shows the equal crystallite size of 1 and 2 h ball milled that have similar reaction yield.[30]

Mohamed et al. (2010) investigated that the platinum dropped nickel oxide was synthesized by the powder mixing method. This method used nickel (II) nitrate hexahydrate dissolved in DI water when the solution was dried and become dried gel of NiO. The platinum powder and nickel oxide powder was milled using roll mill for 2 h and calcine at 400, 500, 600 or 700 °C for 3 h. It was observed that the particle size directly proportional with temperature using calcination. Catalysts were tested in CO_2 hydrogenation. Pt:Ni catalyst of atomic ratio 0.1:1 and using 600°C in calcination for 3 h shows the highest conversion at 89% and CH_4 formation at 89%. Active phase is nickel oxide cubic (NiO cubic) phase that was specified by XRD analysis. From SEM analysis shows that the catalyst particle size was from 89 to190 nm which is a slightly definite cubical shape [31].

Shin et al. (2014) studied Boron–CeO_2 hybrid materials that were prepared by dry and wet ball milling. Materials were characterized by SEM, X-ray, XRD, FT-IR and XPS. They were tested and investigated in CO Oxidation activities of material. The large size boron is covered by much smaller CeO_2. Boron is oxidized at the interface via $2B+6CeO_2 \longrightarrow B_2O_3 + 3Ce_2O_3$. For the wet-milled B–$CeO_2$ hybrid material for 1:1 ratio by weight show $1.1x10^{-14}$ mol gcat $^{-1}s^{-1}$ of the oxidation rate at 400°C in the 2nd run. The 10% CO conversion temperature (T10%) appears at 305 °C. T10% for just CeO_2 was found at above 450°C, while only boron itself, there was no Co oxidation activity founded below 900°C. The hybridization of boron and Ce_3O_2 lead to drastic CO oxidation enhancement of the hybrid material that is attributed to oxygen defects and balanced oxidation states of Ce created. The oxidation state of Ce changed from+4 to +3 after ball-milling are confirmed by XPS binding energies at Ce 3d O1s [32].

Zhang et al. (1997) described the synthesis of Ni-CeO_2 catalysts for ethanol steam reforming by easy ball-milling process that used skeletal Ni and powder CeO_2 as precursors and compared to a Ni/CeO_2 catalysts synthesized by a impregnation

method. The Ni-CeO_2 catalysts were characterized by BET, XRD, TPR, TEM. Ni-CeO_2 catalyst that was prepared by ball-milling process has high Ni active surface area case in favors H_2 production. It gives a yield of 45 mol_{H2} mol_{Ni}^{-1} h^{-1}at 350°C and highly stable. Because the nanoconfinement of nickel particles and strong metal-support interaction. Ethanol conversion remains approximately 90% after 2 h thermal treatment at 700 °C have passed. This catalyst shows anti-coke deposition due to the presence of abundant surface oxygen, when investigated in stability test in ethanol steam reforming for 35 h, it shows a good stability of the catalyst [33].

2.3 solid state reaction

The synthesize solid have several methods. In the preparation of solid state is difficult because the thermodynamic is not stable. Solid state reaction is prepared by the single phase compounds. This synthesis method is the oldest, simplest, and most widely used to mix the powder reactants together that can be compressed into pellets or other shape, then calcination for a long time. It has been well aware that the solids do not react with another at room temperature and it is important to heat them up to the higher temperatures (1000 to 1500°C) in order to initiate the reaction at an appreciable rate. However, there is some information from the research suggest that this solid-state reaction phenomenon seem to taken little notice. These studies have demonstrated that the solid-state interaction not only can occur at high temperature but also at ambient temperature. And it occurs not only in vacuum, but also in a moist atmosphere [34]. Although they seem to be well-mixed at the level of individual particles, the reactants are very inhomogeneous in the atomic level so that the internal reaction in the method is slow. It is because that the large amount of mixing of atoms in particles is required. The solid state, liquid or gas phase transport brings together atoms of the variant elements to form the desired product [6]. The formation of homogeneous solid phase are demonstrated in Table 2.2 based on the physical state of the reactants and the products.

Table 2.2 The formation of homogeneous solid phase

Type	Reaction			
Type I	A(s)	⟶	B(s) + C(g)	(4)
Type II	A(s) + B(s)	⟶	C(s)	(5)
Type III	A(s) + B(s)	⟶	C(s) + D(g)	(6)
Type IV	A(s) + B(g)	⟶	C(s)	(7)
Type V	A(s) + B(g)	⟶	C(s) + D(g)	(8)
Type VI	A(s)	⟶	B(g) + C(g)	(9)

Type I; the reaction of this type can be either endothermic or exothermic. However, studies seem to give more attention on endothermic reaction that is the dehydration of the metal salt hydrate and the decomposition of the metal carbonates. For example, the decomposition of calcium carbonate (10). Crystal lattice solid or crystal structure appears in the decomposition product of the metal hydrates. The new phrase occurs when the dehydration of crystalline hydrate forms are a mostly unregulated products.

$$CaCO_3(s) \longrightarrow CaO(s) + CO_2(g) \qquad (10)$$

Type II; reactions in this type, the atom have limited movement into solid phrase. The reaction relies on the diffusion of reactants over the product layer. The reaction rate resulted from the transfer rate of atoms or ions over the product layer, using the fine particles of the reactants lead to abridged of diffusion. Therefore, the new form phase has low crystalline and a high defects. For example

$$ZnO(s) + Al_2O_3(s) \longrightarrow ZnAl_2O_4(s) \qquad (11)$$

Ways to improve the efficiency which take less time to build products of solid state reaction are listed below.

- Using the reactant with high surface area
- Preparation of compounds over single phase precursor
- During crystallization, adding impurities in solid
- A new form solid is resulted from the coupling effect
- Using high energy radiations

Li et al. (1997) reported preparation by solid-state reaction of HZSM-5 with $MgCl_2$ at 327°C to study the effect of different amount of magnesium on Mg-ZSM-5 zeolite catalysts. The comparison by XRD between Mg-ZSM-5 zeolite catalysts sample and HZSM-5 zeolite show the same structure and crystallinity. From the analysis of NH_3-TPD and IR of pyridine adsorption show that when magnesium amount increases in zeolite catalysts, the result in their Bronsted acid sites decreased and Lewis acid sites slightly increased. A series of Mg-ZSM-5 zeolite catalysts were tested in alkylation of toluene with methanol at 600 K. the modified zeolite catalysts show initial activity and lifetime better than the HZSM-5 zeolite and also increasing para-selectivity to a level of 80-90% [34].

Cubeiro et al. (1999) study to effect of K promoter on Fe/Al_2O_3 catalysts in CO and CO_2 hydrogenation reaction at 553–563K and 1.2MPa, using three preparations of the catalysts which are impregnation, precipitation and physical mixing of the support with Fe oxide to investigate different degrees of interaction between Fe and the support. This study found that, in some cases the transformation of Fe are modified when adding K, also accelerate the reduction–carburization process and increase the reoxidation during the carbon oxide hydrogenation reactions. In all catalysts show similar of activity. However, selectivity reveals small but reliable differences, which could be interrelated to the Fe phase composition in catalysts. Higher proportions of

non-carbided Fe increase more methane, alkanes and internal alkenes formation [14].

Table 2.3 Advantage and disadvantage of solid state reaction

Advantage	Disadvantage
1. The simplest 2. Cheaper and convenient 3. use less solvent and contamination 4. give high yield of product	1. irregularly disperse metallic over support 2. decompose of material

2.4 Active element for methanation reaction, CO hydrogenation and CO_2 hydrogenation

2.4.1 Metal-base catalysts

Normally, metal-based catalysts are used as active phase in catalysts for methanation reaction, CO hydrogenation and CO2 hydrogenation such as Ni [1, 2, 4, 8, 9, 11-13], Fe [14] ,Ru [13, 14], Co [13, 15-17],and Pt [13].

Das et al. (2008) investigate the synthesis of cobalt catalysts with different loadings and supports for CO_2 hydrogenation reaction at 533K which were studied by in situ DRIFT spectroscopy. The Series of silica, alumina, magnesia, titania, niobia, zirconia, and ceria supported cobalt were characterized by Ultraviolet visible near-infrared (UV–vis–NIR) spectroscopy and X-ray diffraction (XRD). the ceria supported catalysts with 15 and 20 wt.% cobalt showed the best conversions, CO_2 conversion

and methane yield as respectively followed : CoCe > CoMg ≈ CoAl > CoZr≈ CoTi > CoSi > CoNb [35].

Park et al. (2009) reported Pd–Mg/SiO_2 was prepared by a reverse microemulsion synthesis for carbon dioxide methanation at 450°C. The catalyst consists of Pd with the 5 to 10 nm in size of particles, distributed within an amorphous oxide of Mg and Si that found after calcinnation. The catalytic activity and selectivity of the Pd–Mg/SiO_2 catalyst were compared to several other catalyst preparations. The Pd–Mg/SiO_2 catalyst shows better than 95% selectivity to CH_4 at a carbon dioxide conversion of 59%. While Pd/SiO_2 have activity only for CO_2 reduction to CO, and the Mg/SiO_2 are relatively inactive [10].

It is well known that noble-metal catalysts, such as Ru-based catalysts, are excellent for CO methanation. However, because of their high costs, Ru is not a commercial catalyst in the industry. Co-based catalysts are well tolerates to harsh environments, but it gives poor selectivity. Ni-based catalysts are greater than Co-based and Fe-based catalysts because of their high catalytic activity, high CH_4 selectivity, and cheap price. With these reasons, Ni-based catalysts are capable as good industrial catalysts. So, Ni-based catalysts are popular to use is used as active phase in catalysts for methanation reaction, CO hydrogenation and CO_2 hydrogenation.

Zhang et al. (2009) studied NiO/Al_2O_3 catalysts that were modified with SiO_2, ZrO_2 and MgO for methanation of CO .the catalyst were prepared by a modified grinding-mixing method and characterized using XRD, TEM, N_2 adsorption-desorption isotherms, H_2-TPR, H_2-TPD, Raman spectroscopy, and XPS. The activity of a modified NiO/Al_2O_3 catalysts with MgO result better than both NiO/ZrO_2-Al_2O_3 and NiO/SiO_2-Al_2O_3 in the methanation reaction, using temperature range 300–700°C. NiO/MgO-Al_2O_3 catalyst gives 99.6% at 500°C because it has the significantly weakened Ni–Al interactions and consequently reduction of the catalyst at low temperatures. So,

MgO promotes NiO/Al_2O_3 catalyst easier to reduce, leading to generation of more free nickel-oxide species on the catalyst surface [2].

2.4.2 Nickel

Nickel is metal that was classified in transition metal and having atomic number 28. Ni is chemical symbol of nickel. Two electronic configurations of Ni are [Ar] 4s2 3d8 and [Ar] 4s1 3d9. Nickel has the crystalline structure as a face centered cube (FCC) and the lattice parameter of 0.352 nm, having an atomic radius of 0.124 nm. And more data of Nickel were show in Table 2.4.

Common oxidation state of Nickel are Ni^0, Ni^+, Ni^{2+} and exotic oxidation states such as Ni^{2-}, Ni^{1-}, and Ni^{4-}. Nickel has +2 valance states for the major common oxidation state.

Nickel (0): It is a highly toxic liquid at ambient temperature and become nickel and carbon monoxide when it is heated.

$$Ni(CO)_4 \rightleftharpoons Ni + 4CO \qquad (2.10)$$

Nickel (I): compounds are rare, for example the tetrahedral complex $NiBr(PPh_3)_3$. That is complex is oxidized in water.

Nickel (II): complexes are common anions, for example the sulfide, sulfate, carbonate, hydroxide, carboxylates, and halides. The nickel salts (chloride, nitrate, and sulfate) can dissolve in water and becomes green solutions (metal aquo complex $[Ni(H_2O)_6]^{2+}$). The tetracoordinate nickel (II) compounds consist of tetrahedral and square planar geometries. The tetrahedral compounds are paramagnetic but the square planar compounds are diamagnetic.

Nickel (III): can be found with fluoride and oxides form that is nickel (III) oxide.

Nickel (IV): transpires with fluoride and oxides which is the mixed oxide BaNiO. It is used as the cathode in rechargeable batteries.

Table 2.4 Information of nickel.[36]

Physical properties	
Phase	Solid
Melting point	1728 K(1455 ^{0}C, 2651^{0}F)
Boiling point	3003 K (2730 ^{0}C, 4946 ^{0}F)
Density near r.t	8.908 g-cm^{-3}
Liquid, at m.p.	7.81 g-cm^{-3}
Heat of fusion	17.48 kJ-mol^{-1}
Heat of Vaporization	379 kJ-mol^{-1}
Molar heat capacity	26.07 J-mol^{-1}-k^{-1}
Atomic properties	
Oxidation states	4, $^{(1)}$3,2,1, $^{(2)}$-1 (a mildly basic Oxide)
Electronegativity	Pauling scale: 1.91
Lionization	1st: 737.1 kJ- mol^{-1}
Energies	2nd: 1753.o kJ- mol^{-1}
	3rd: 3395 kJ- mol^{-1}
	empirical: 124 pm
Atomic radius	124±4 pm
Covalent radius	
Van der waals radius	163 pm
General properties	
Name, symbol	nickel, Ni
Appea	lustrous, metallic, and Silver with a gold tinge

จุฬาลงกรณ์มหาวิทยาลัย
Chulalongkorn University

Table 2.4 Information of nickel. (Cont'd)

Nickel in the periodic table	
Atomic number Standard atomic	28
Weight Element	58.6934(4)
Category Group, block	transition metal group 10, d-block
Period	period 4
Electron	(Ar) $3d^8\ 4s^2$ or
Configuration	(Ar) $3d^9\ 4s^1$ (see text)
Per shell	2,8,16,2 or 2,8,17,1
Miscellanea	
Oxidation states	4, $^{(1)}$3,2,1, $^{(2)}$-1 (a mildly basic Oxide)
Electronegativity	Pauling scale: 1.91
Lionization	1st: 737.1 kJ- mol^{-1}
Energies	2nd: 1753.o kJ- mol^{-1}
	3rd: 3395 kJ- mol^{-1}
	empirical: 124 pm
Atomic radius	124±4 pm
Covalent radius	
Van der waals radius	163 pm

จุฬาลงกรณ์มหาวิทยาลัย
Chulalongkorn University

2.5 Alumina

Aluminas are the most common commercial carriers because of their excellence thermal stability and wide range of chemical, physical and catalytic properties such as coating, catalysts, catalyst supports, sorbent and ceramics.

The structures of alumina are classified to three classes:

Classes 1: Aluminum trihydroxides ($Al(OH)_3$): Gibbsite, Bayerite, and Nordstrandite are Three crystallized in $Al(OH)_3$. The Gibbsite is the main part that used calcination change to corundum for aluminum manufacture. The crystallized of $Al(OH)_3$ may be took about to amorphous hydroxide synthesis under condition of pH and temperature.

Classes 2: Aluminum oxyhydroxides (AlO(OH)):The $AlO(OH).xH_2O$ compose of boehmite, and diaspora. The third form occurs from boehmitewhich has specific property, called pseudoboehmite or microcrystalline boehmite [8].

Classes 3: Aluminum oxides (It is distinguished between transition aluminas and alpha alumina) [37].

The alumina vary over wide ranges of surface area of 0.5-600 m^2/g, pore size and size distribution, and acidity and high melting point (over 2000°C). So, it is suitable for used to desirable for the support. Due to, it has the high melting point, so it has distinguished characteristics for separating particles of a catalytic substance from each other and as a support and as thermal stabilizer of catalyst. Dilute, support, and disperse the precious metals is the role of alumina. The support also stabilizes the metastable dispersion of small metallic crystallites on the surface of the alumina that helps against agglomeration and sintering. For case of a deposit of the quantity of an active phase that is lower than the adsorption capacity of the alumina support. It also displays a role in the macroscopic distribution of the crystallites thus, it is possible to obtain a homogeneous.

The phase transformation of alumina is several such as the gamma (γ) alumina, eta (η), kappa (κ), chi (χ) and delta (δ). That it is Depend on Calcination or heating in air to different temperatures and starting matter such as gibbsite,

boehmite, determines the final crystal structure, chemical and physical properties .show in fiture1 From Figure 2.4 that summarizes the pathways of gibbsite thermal decomposition. Gibbsite decomposes convert to oxide when heat up in air above the temperature of 300ºC.

Nowadays, γ-Al_2O_3 is the most widely used commercial structure used as a support for metal catalyst.

Liu et al. (2012) reported the effect of La and Ru promoters and the effect of reduction conditions in Co/γ-Al_2O_3 catalysts that prepare by co-impregnation. La promoter gave the highest level of activity. The activity was resulted in the degree of reduction that CoO change to Co metal. The reduction was strongly influenced cause by promoters and the reduction conditions required to activate the catalyst. Reduction to Co metal was improved by using 400ºC for 10 h in reduction with reach to 74% additional CoO reduction achieved compared. From this research show that the key to the improved methanation activity was the extent of Co-oxide reduction to Co metal [38].

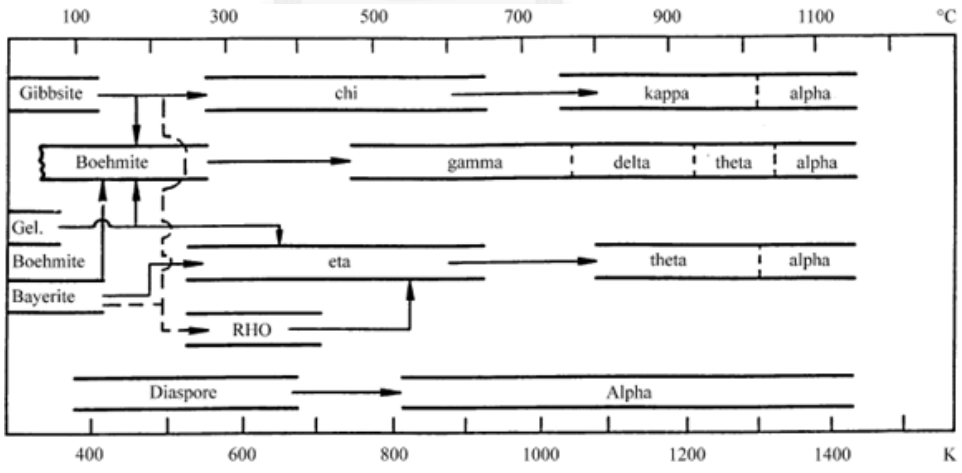

Figure 2.4 Decomposition sequences of aluminum hydroxides [9].

2.6 The effects of promoters on the properties of Ni/ γ-Al_2O_3 catalysts in methanation reaction, CO hydrogenation and CO_2 hydrogenation.

With many advantages, Ni/ γ-Al_2O_3 catalysts has been widely used and studied, especially with these two processes about hydrogen production that are steam reforming of methane and purification of obtained hydrogen from traces of carbon oxides. With these advantages and good price, Ni-based catalysts are suitable and promising as good industrial catalysts. However, conventional Ni/ γ-Al_2O_3 catalysts deactivate easily because sintering of Ni particles and coke deposition during the exothermic methanation reaction. The addition of Ni content can increase their catalytic activities but may accelerate the deactivation of the catalyst in long-term during operation. So researches and development have added the second metal or promoter as a way to solve the problem of deactivation [1, 2, 39].

There are two kinds of promoter; textural and chemical. Firstly, Textural promoters are added with the goal to improve the physical properties, For example, to facilitate the preparation of well-dispersed catalytic phases and maintain their well-dispersed state during reaction conditions. Chemical promoters are added to improve the activity and selectivity of the catalytic phase. Generally, chemical promoters consist of alkali, alkaline earth, metal oxide, and noble metals.

Recently, there have been researches which study about the effects of promoters on the properties of γ-Ni/Al_2O_3 catalysts in methanation reaction, CO hydrogenation and CO_2 hydrogenation.

Znak et al. (2010) studied added cerium, lanthanum and zirconium in to nickel/alumina catalysts for CO and CO_2 hydrogenation. The catalysts were prepared by impregnation of nickel/alumina that using synthesize from precipitation method. A series of Ni/Al_2O_3 catalysts were characterized by temperature-programmed reduction, X-ray diffraction, TP desorption of pre-adsorbed hydrogen, adsorption of O2 and its TP hydrogenation, thermal effect of O_2 adsorption, adsorption of CO and its TP desorption and TP hydrogenation. The result from TP desorption of H_2 gas and

TP hydrogenation of pre-adsorbed O_2 gas show the promoter do not to modify the state of H_2 and O_2 adsorbed on nickel. Meanwhile, the TP desorption of pre-adsorbed CO show that Zr, Ce and La significantly promote dissociation of CO and demonstrate to emphasize on small effect of La and Ce on the dissociation of CO. Which relate and can be used to explain, the catalytic performance test show that Zr, Ce and La considerably increase conversion of CO and CO_2 to methane [39].

Zhao et al. (2012) investigated different of Mn content that vary from 1-3 wt% to promote Ni/Al_2O_3 catalysts. The promoted Ni/Al_2O_3 with Mn were prepared by co-impregnation method and characterized by N_2 physisorption, XRD, H_2-TPR, SEM and TEM. Their catalytic activities were test in a fixed-bed reactor for methanation reaction. From BET and XRD show that addition of manganese to Ni/ Al_2O_3 catalysts can increase the catalyst surface area and average pore volume but decrease NiO crystallite size. Moreover, Mn makes Ni/Al_2O_3 easier to reduce. This result leading to higher activity and stability compare with non-promoted Ni/Al_2O_3. Promoted Ni/Al_2O_3 with 1% Mn show the most stable under high temperature (450 °C). Adding 3% of Mn to Ni/ Al_2O_3 catalysts gives t highest active at 250-300 °C. Ni-Mn/ Al_2O_3 lead to slightly change CH_4 formation rate and the product distribution but temperature of reaction show more important role [8].

Hu et al. (2012) study several parameters of the Ni/Al_2O_3 catalysts in CO Methanation. The parameters are different commercial Al_2O_3 supports, varying NiO and MgO loading, calcination temperature, space velocity, H_2/CO ratio, reaction pressure, and time that all parameter have effect with the properties of NiO species in the catalyst. 20% NiO on the S_4 Al_2O_3 support (>95%, spherical shape, Gongyi Huayu Alumina Co. Ltd., China) and using calcination at 400 °C can occur a high reducible of NiO. This lead to generate of highly active Ni^0 particles. Moreover, the addition of MgO (2 wt %) increase conversion and CH_4 selectivity at low GHSV of 30,000 mL/g·h, at a high pressure of 3.0 MPa, and a molar ratio of H_2/CO more than 3:1. Because it show enhance the resistance to the carbon deposition, so significantly increasing the stability of the Ni catalysts [1].

จุฬาลงกรณ์มหาวิทยาลัย
Chulalongkorn University

Table 2.5 Summary of Literature reviews catalysts in methanation reaction, CO hydrogenation and CO_2 hydrogenation that relate in this research

No. Ref.	Reaction	Works and studies	Preparation method	Active phase	Promoter	Results
1	CO Methanation	Effect of different commercial Al_2O_3 supports, varying NiO and MgO loading, calcination temperature, space velocity, H_2/CO ratio and reaction pressure	impregnation	Ni	Mg	20% NiO on the S_4 Al_2O_3 support (>95%, spherical shape, Gongyi Huayu Alumina Co. Ltd., China) and using calcination at 400 °C gave the best performance. The addition of MgO (2 wt %) increased conversion and CH_4 selectivity at low GHSV of 30,000 mL/g•h, high pressure of 3.0 MPa, and a molar ratio of H_2/CO more than 3:1
2	methanation of CO at 500°C	The modification of NiO/Al_2O_3 with SiO_2, ZrO_2 and MgO	grinding-mixing	Ni	SiO_2, ZrO_2 and MgO	$NiO/MgO-Al_2O_3$ was the best catalysts, giving 99.6% of CO_2 conversion Ni–Al interactions of $NiO/MgO-Al_2O_3$ was weak. The reduction occurred at low temperatures. So, it was easier to reduce.

Table 2.5 Summary of Literature reviews catalysts in methanation reaction, CO hydrogenation and CO_2 hydrogenation that relate in this research. (cont'd)

No. Ref.	Reaction	Works and studies	Preparation method	Active phase	Promoter	Results
9	CO and CO_2 hydrogenation reaction at 553–563 K	effect of K promoter on Fe/ Al_2O_3 catalysts	impregnation, precipitation and physical mixing	Fe	K	Fe-K/Al_2O_3 showed lower proportion of carbided Fe in fresh catalysts leading to higher methane selectivity and higher alkanes/alkenes
23	CO_2 hydrogenation	The effect of platinum dropped in nickel oxide and Calcine- temperature at 400, 500, 600 or 700 °C	powder mixing	Ni	Pt	Pt:Ni catalyst of atomic ratio 0.1:1 and using 600°C in calcination for 3 h showed the highest conversion at 89% and CH_4 formation at 89%.

Table 2.5 Summary of Literature reviews catalysts in methanation reaction, CO hydrogenation and CO_2 hydrogenation that relate in this research. (cont'd)

No. Ref.	Reaction	Works and studies	Preparation method	Active phase	Promoter	Results
30	methanation	The effect of La and Ru promoters and the effect of reduction conditions in Co/γ-Al_2O_3 catalysts	co-impregnation	Co	La and Ru	La promoter gave the highest level of activity Key to the improved methanation activity was the extent of Co-oxide reduction to Co metal
31	CO and CO_2 hydrogenation	Effect of La, Zr and Ce on Ni/Al_2O_3 catalysts	precipitation method	Ni	La, Zr and Ce	Cerium, Lanthanum and Zirconium promoted dissociation of CO which led to the increasing catalytic activity of NiO/Al_2O_3 catalysts. La promoter was the best

CHAPTER III

EXPERIMENTAL

3.1 Chemicals

Chemicals and suppliers used in this research are displayed as followed:

Table 3.1 Chemicals used for synthesis of the catalysts

Chemicals	Suppliers
Fine gibbsite	Merck
Nickel (II) nitrate hexahydrate 98%	Sigma-Aldich
Cerium (III) nitrate hexahydrate 99.5%	Acros
Manganese(II) acetate tetrahydrate 99%	Aldich
Potassium nitrate	BDH chemical
Magnesium nitrate hexahydrate 99.0%	BDH chemical
Lanthanum(III) nitrate hexahydrate 99.0%	Himedia

จุฬาลงกรณ์มหาวิทยาลัย
Chulalongkorn University

3.2 Materials preparation

3.2.1 Catalyst preparation by incipient wetness impregnation

A tube furnace at 500°C was used to calcine gibbsite for three hours to acquire the γ-alumina (Al_2O_3) support. After that, aqueous solution of nickel nitrate and the promoter were mixed and impregnated on γ-Al_2O_3. Then, the catalyst samples were dried overnight at 110°C. Finally, calcination occurs at 500°C for 3 h in air flow. Each catalysts sample prepared has 20 percent of nickel with 1 percent of difference types of promoter (K, Mn, La, Ce or Mg).

3.2.2 Catalyst preparation by solid state reaction

The preparation of solid-state reaction method used the mechanical mixture of nickel nitrate, gibbsite, and different promoters (KNO_3, $(CH_3COO)_2Mn$, $La(NO_3)_3$, $Ce(NO_3)_3$ or $Mg(NO_3)_2$). Ni loading of 20 wt% was modified by 1 wt% promoter. First of all, the amount of nickel nitrate, gibbsite, and one type of promoter were mixed in an agate mortar. Later, the mixed samples were dried at 110°C for overnight. Lastly, the sample of catalysts were calcined in a tube furnace in 95 ml/min of air at 500°C, heating rate of 10°C/min and this temperature was hold for 3 h.

For catalytic preparations by solid-state reaction with dry ball mill used the same precursor as the previous preparation. All these precursor and alumina ball with 3.3 ml diameter were loaded in HDPE bottle of 100 ml. After that, the HDPE bottle was rolled at the speed of 70 rpm. Substances that are separated from alumina ball and were mixed in an agate mortar. Then, the mixed materials were dried at 200°C for 6 h and were calcined at 500°C for 3 h.

3.3 Catalysts characterization

จุฬาลงกรณ์มหาวิทยาลัย
Chulalongkorn University

3.3.1 X-ray diffraction (XRD)

X-ray diffraction (XRD) were characterized to determine bulk phase of catalystsby SIEMENS D 5000 that use CuK_α of catalysts radiation with Ni filter in scanning range from 10 to 90 degrees of 2θ at resolution 0.4°.

3.3.2 N_2 physisorption

Nitrogen physisorption was analyzed by the multiple point method, used to determine the BET surface area, pore size diameter, pore volume. The amount of nitrogen gas was measured for calculated the size distribution and the surface according to Barret-Joyner-Halenda (BJH) and Bruanuer-Emmett-Teller (BET) by a Micrometrics ASAP 2020.

3.3.3 Scanning electron microscopy (SEM)

The morphology and agglomeration of the catalyst particles were analyzed by JEOL mode JSM-5800LV of scanning electron microscopy technique

3.3.4 X-ray photoelectron spectroscopy (XPS)

X-ray photoelectron spectroscopy (XPS) was used to analyze the composition on the surface of catalysts that measured by AMICUS spectrometer using a Mg K-α X-ray radiation at 15 kV with the current of 12 mA. The pressure analysis chamber should be less than 10^{-5} Pa.

3.3.5 Temperature-programmed reduction (TPR)

Hydrogen temperature-programmed reduction (H_2-TPR) was used to study the reduction behavior of catalysts that measure by Micrometrics Chemisorb 2750 system. Firstly, 0.1 g of catalyst sample was packed in a quartz U-tube reactor. then, the catalysts sample will be heated up to 500°C in flow of nitrogen gas and held at 500°C for 30 minute and next cooled down to room temperature. After that, the catalysts will be heated up from room temperature to 800°C with 25 ml.min^{-1} of 10% H_2 in Ar. The thermal conductivity detector (TCD) was used to determine the amount of hydrogen gas, used to reduce the catalysts.

3.3.6 Carbon mono oxide chemisorption

Carbon mono oxide chemisorption was characterized by a Micrometritics Chemisorb 2750, as well as, ASAP 2101CV.3.00 software to measure the amount of active site and the dispersion of metal particles. Firstly, using 0.1 g of catalyst sample was packed in U-tube glass reactor. Next, the catalysts sample was reduced at a 50 mL•min^{-1} of flow rate in of H_2 gas. The catalyst was heated up to 400°C and held at 3 h and cool down with He gas. When the catalysts sample was cooled to room temperature, injecting 20µl of CO gas in to the catalyst sample until it is not

adsorbed. The gas chromatograph with thermal conductivity detector (TCD) was used to determine to amount of injected carbon mono oxide gas.

3.3.7 Particle size analysis

The particle size was analized by a Zetasizer with nano series model from Malvern Instruments Ltd., Worcestershire, England. The catalysts sample was dispersed for 5 mins in DI water by sonication. Averages of three independent measurements were taken.

3.4 Reaction in carbon dioxide hydrogenation

3.4.1 Materials

Table 3.2 Gas materials are used to catalytic activity test.

Chemical and Regents		Supplier
High purity grad nitrogen	(99.99 vol.%)	Thai industrial Gases Limited
High purity grad hydrogen	(99.99 vol.%)	Thai industrial Gases Limited
Carbon dioxide in hydrogen	(8.80 vol.%)	Thai industrial Gases Limited

3.4.2 Apparatus

The CO_2 hydrogenation system includes a reactor, an electrical furnace, a temperature controller, a gas controlling system, and a gas chromatography.

3.4.2.1 Reactor

The reactor was made from a quartz tube that inside diameter is 9 mm. The 0.05 g of catalyst sample was packed between quartz wool layers.

3.4.2.2 Electrical furnace

The reactor was supplied by heat from the electrical furnace. The reactor use electricity at 220 volt that can operate in room temperature of 800°C.

3.4.2.3 Temperature controller

This system composed of a thermocouple that was connected with temperature controller model no. SS2425DZ to detect temperature of the reactor. The temperature controller can be adjusted within the range 0-800°C at 220 volt.

3.4.2.4 Gas controlling system

The reactant gas was controlled by a pressure regulator. The metering valves were employed to adjust the gas flow rates and on-off valve.

3.4.2.5 Gas chromatography

The feed and product streams' gas composition were analyzed by The Thermal conductivity detector (TCD) with Shimadzu GC8A (molecular sieve 5 Å) gas chromatograph. The operating conditions are shown in the Table 3.3.

จุฬาลงกรณ์มหาวิทยาลัย
CHULALONGKORN UNIVERSITY

3.4.3 The CO_2 hydrogenation procedures

The carbon dioxide hydrogenation reaction was tested in a quartz micro reactor, in 0.05 g catalyst sample was packed. Firstly, the catalyst was reduced by using 50 ml/min hydrogen gas at 400°C for 4 h. Then, the gas was changed to 21.2 ml/min of total flow rate of 8.8% CO_2 in H_2, with the H_2/CO_2 ratio of 10/1 when it reached 500°C. The total pressure was at 1 atm. The outlet gases were analyzed by gas chromatograph equipped using TCD to separate methane (CH_4), carbon dioxide (CO_2) and carbon monoxide (CO).

Table 3.3 The operating conditions for GC

Gas Chromatograph	Shimadzu GC-8A
Analyzed gas	HydrocarbonC_1-C_4 ,CO, CO_2, H_2
Detector	TCD
Column	Molecular sieve 5 Å
Column material	SUS
Length	2 m
Outer diameter	4 mm
Mesh range	60/80
Maximum temperature	350°C
Carrier gas	He (99.999%)
Carrier gas flow	40 ml/min
Column gas	He (99.999%)
Column gas flow	40 ml/min
Column temperature initial (°C)	70
Column temperature final (°C)	70
Detector temperature (°C)	100
Injector temperature (°C)	100
Current (mA)	80

จุฬาลงกรณ์มหาวิทยาลัย
Chulalongkorn University

CHAPTER IV
RESULTS AND DISCUSSION

This chapter is divided into two parts. Part (4.1) illustrates the effect of different types of promoter (K, Mn, La, Ce, and Mg) on the Ni/Al_2O_3 catalysts which were prepared by the incipient wetness impregnation. Part (4.2) illustrates the effect of the selected promoters (from part 1) on Ni/γ-Al_2O_3 catalysts by solid-state reaction with and without dry ball mill and the results were compared to the ones prepared by conventional impregnation method.

The characterization of catalysts by various techniques including XRD, N_2 physisorption, H_2-TPR, SEM, XPS, and CO chemisorption were also presented. All the catalysts were tested in the CO_2 hydrogenation at 500 ºC and atmosphere pressure. The reactants consisted of H_2 and CO_2 in 10:1 proportion as reactant feed gas. The catalyst performances in the CO_2 hydrogenation are explained in this part.

4.1 Effect of promoter (K, Mn, La, Ce, and Mg) on the Ni/Al_2O_3 catalysts prepared by impregnation

จุฬาลงกรณ์มหาวิทยาลัย
Chulalongkorn University

The catalyst nomenclatures are as shown below:

imp_Ni/Al_2O_3 presents the catalysts which were prepared from the mixture of nickel nitrate and gibbsite by incipient wetness impregnation

imp_Ni-Ce/Al_2O_3 presents the catalysts which were prepared from the mixture of nickel nitrate, cerium nitrate and gibbsite by incipient wetness impregnation

imp_Ni-K/Al_2O_3 presents the catalysts which were prepared from the mixture of nickel nitrate, potassium nitrate and gibbsite by incipient wetness impregnation

imp_Ni-La/Al_2O_3 presents the catalysts which were prepared from the

mixture of nickel nitrate, lanthanum nitrate and gibbsite by incipient wetness impregnation

imp_Ni-Mg/Al_2O_3 presents the catalysts which were prepared from the mixture of nickel nitrate, magnesium nitrate and gibbsite by incipient wetness impregnation

imp_Ni-Mn/Al_2O_3 presents the catalysts which were prepared from the mixture of nickel nitrate, manganese acetate and gibbsite by incipient wetness impregnation

4.1.1 Catalysts characterization

4.1.1.1 X-ray diffraction (XRD)

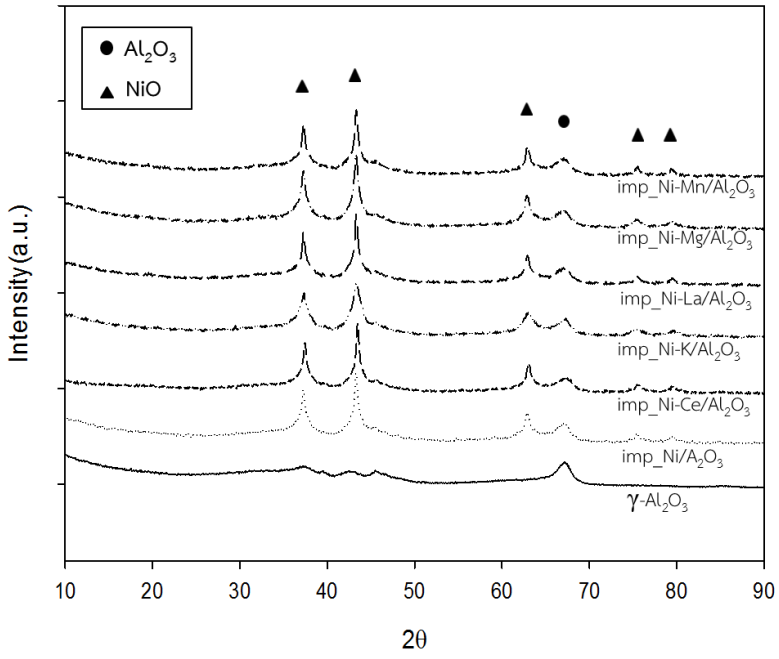

Figure 4.1 The XRD patterns of support and Ni/Al_2O_3 catalysts with different promoters

The XRD patterns of Ni/Al_2O_3 catalysts with different types of promoters are shown in Figure 4.1. The XRD pattern of all Ni-based catalysts exhibited similar

characteristic peaks of NiO at 2θ = 37.3°, 43.3°, 62.9°, 75.3°, and 79.5° (JCPDS 47-1049). The XRD pattern of support displays major peak at 2θ = 67.0° indicating the presence of γ-phase crystalline of alumina. Moreover, small peaks were found around 2θ = 43°, where a small amount of χ-phase crystalline occurred in alumina support. In terms of doping catalysts, the XRD peaks corresponding to potassium, manganese, lanthanum, cerium or magnesium species were not detected because they were smaller than the detection limit of the XRD or due to the insufficient amount present. It is possible that the added promoters on Ni/Al_2O_3 catalysts had a highly dispersion and formed small particles on the catalyst surface.

The average crystallite sizes of NiO were calculated by the Scherrer's equation using the full width at half maximum of the XRD peak at 2θ = 43.3°. Table 4.1 shows the NiO crystallite sizes of all Ni-based catalysts, which were ranged between 6.5 to 14.8 nm. Ni/Al_2O_3 catalysts promoted by Ce, La, Mg, and Mn resulted in a decrease of the NiO crystallite size. The NiO crystallite sizes of K promoted Ni/Al_2O_3 catalyst significantly decreased from 14.8 to 6.5 nm. It suggests that addition of the promoter resulted in the formation of smaller NiO crystallite sizes on the support, leading to the highly dispersion of Ni metal on alumina surface [40].

จุฬาลงกรณ์มหาวิทยาลัย

Table 4.1 Average NiO crystallite size of Ni-based catalysts with different promoters

Sample	Average NiO crystallite size from XRD (nm)
imp_Ni/Al_2O_3	14.8
imp $Ni\text{-}Ce/Al_2O_3$	14.3
imp $Ni\text{-}K/Al_2O_3$	6.5
imp $Ni\text{-}La/Al_2O_3$	14.5
imp $Ni\text{-}Mg/Al_2O_3$	13.1
imp $Ni\text{-}Mn/Al_2O_3$	13.8

4.1.1.2 Nitrogen physisorption

Nitrogen physisorption was used to examine textural properties of the supports and catalysts. BET (Brunauer-Emmett-Teller) method was used to determine the surface area of catalysts. The BET surface area, pore volume and average pore size diameters of the catalysts samples are summarized in Table 4.2. Pure γ-Al_2O_3 support had the surface area of 162.7 m^2/g and these of the Ni-based catalysts were ranged between 93-117 m^2/g. Active Ni and promoters can access to the pores of Al_2O_3 supports so that some pores of Al_2O_3 were blocked after impregnation, resulting in lower pore volume and surface area[8, 41]. There were no significant differences in textural properties of the nickel catalysts promoted with potassium, manganese, lanthanum, cerium, magnesium and the non-promoted nickel catalysts.

Table 4.2 Physiochemical of Ni-based catalysts prepared by impregnation methods

Catalyst	BET surface area (m^2/g)	Average pore volume (cm^3/g)	Average pore size diameters (nm)
γ-Al_2O_3	162.7	0.21	3.25
imp_Ni/Al_2O_3	103.1	0.15	3.50
imp_Ni-Ce/Al_2O_3	108.5	0.16	3.44
imp_Ni-K/Al_2O_3	93	0.13	3.50
imp_Ni-La/Al_2O_3	114.1	0.16	3.42
imp_Ni-Mg/Al_2O_3	102	0.15	3.50
imp_Ni-Mn/Al_2O_3	116.7	0.17	3.50

4.1.1.3 Hydrogen temperature program reduction (H_2-TPR)

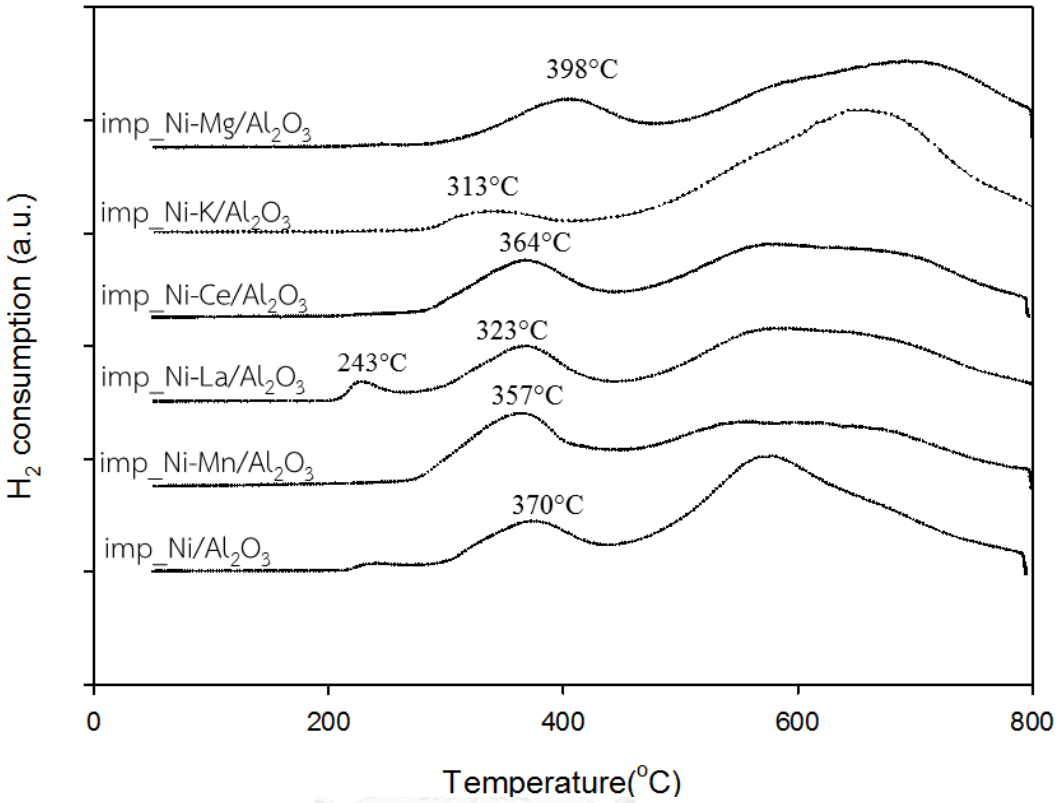

Figure 4.2 The TPR profiles of Ni/Al_2O_3 catalysts with different promoter

จุฬาลงกรณ์มหาวิทยาลัย
Chulalongkorn University

H_2-TPR technique was used to study the reduction behaviors and reducibility of Ni-based catalysts. Metal-support interaction leads to different reducibility of nickel species on the support which can be displayed in the TPR profiles. The results of H_2-TPR are shown in Figure 4.2. The reducible NiO species can be categorized into four types, which are, α, β1, β2, and γ [42, 43]. The α-type is NiO species that the peak located from 180 to 260 °C. Nickel oxides species of α-type have a weak interaction with alumina support which may be a free nickel oxide and bulk NiO. The β-type NiO species have located peaks at 260–500 °C, a mild-temperature, which has a stronger interaction with alumina support than NiO in the α-type. The β-type is further categorized into β1-type and β2-type. β1-type is Ni-rich mixed oxide

phase attributed to the more reducible NiO while β2-type is an Al-rich phase which shows less reducible one. Lastly, γ-type NiO species had the highest temperature peaks at 500–840°C which is a stable nickel aluminate phase ($NiAl_2O_4$). Ni interact strongly with the support is difficult to reduce to Ni^0 species at low temperature [1].

Ni-based catalysts promoted with potassium, manganese, lanthanum and cerium shifted β-type reduction peak to the lower temperature, compared to the non-promoted Ni catalyst, leading to the increasing of α-type and β1-type NiO species. This suggests that, the reduction of NiO was easier when adding these four promoters to the Ni/Al_2O_3. On the other hand, when adding Mg into the Ni/Al_2O_3 displays the shift of β-type and γ-type NiO species peaks towards the right hand side, comparing with the non-promoted one. Thus, this decreases the reducibility at low temperature of NiO species. Because $NiO\text{-}Al_2O_3$ interface occurred to form the NiMg(Al)O mixed oxide and higher interaction between nickel atoms and the neighboring cations[44, 45] as also suggested by Hu et al [1].

H_2 consumption was calculated from peak area of the TPR profiles and the quantity of H_2 gas is related to the quantity of active nickel oxide in catalyst. The TPR results are shown in Table 4.3. The H_2 consumption of the Ni-based catalysts were ranged between 19,550 - 21,978 μmol/g. It can be seen that the promoted Ni catalysts had higher H_2 consumption than the non-promoted one. It suggests that the reducibility of the promoted Ni catalysts increased. The H_2 consumption of $Ni\text{-}K/Al_2O_3$ presented the highest hydrogen consumption.

Table 4.3 H_2 consumption of non-promoted and promoted nickel catalysts

Sample	H_2 consumption (umol/g)
imp_Ni/Al_2O_3	19,550
imp_Ni-Ce/Al_2O_3	19,837
imp_Ni-K/Al_2O_3	21,978
imp_Ni-La/Al_2O_3	20,455
imp_Ni-Mg/Al_2O_3	20,501
imp_Ni-Mn/Al_2O_3	21,101

4.1.1.4 Scanning electron microscopy analyses (SEM)

จุฬาลงกรณ์มหาวิทยาลัย
Chulalongkorn University

The SEM images of the non-promoted Ni/Al_2O_3 catalysts and promoted are shown in Figure 4.3. All nickel catalysts showed non-uniform particle size and shape. It is noticeable on SEM images, the K, Mn promoter can result in the decrease of agglomeration of the catalysts, as well as, smaller particle size than the non-promoted one. But the promotion of Ce, La, Mg on Ni/Al_2O_3 catalysts resulted in more agglomeration of the catalysts.

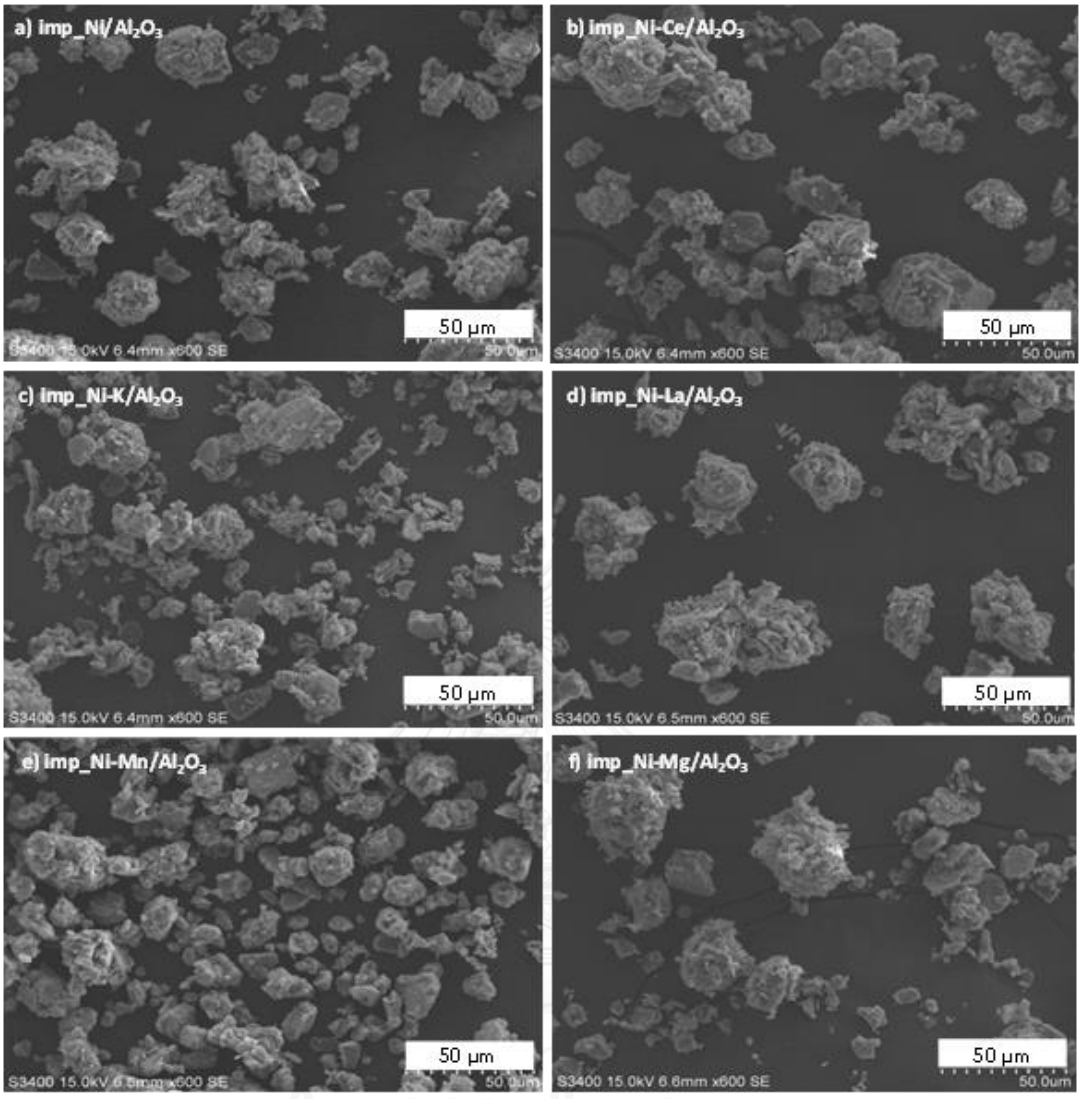

CHULALONGKORN UNIVERSITY

Figure 4.3 The SEM images of Ni/Al_2O_3 catalysts with different type promoters: a) imp_Ni/Al_2O_3, b) $imp\_Ni\text{-}Ce/Al_2O_3$, c) $imp\_Ni\text{-}K/Al_2O_3$, d) $imp\_Ni\text{-}La/Al_2O_3$, e) $imp\_Ni\text{-}Mn/Al_2O_3$ and f) $imp\_Ni\text{-}Mg/Al_2O_3$.

4.1.1.5 Carbon monoxide chemisorption

CO chemisorption was used to determine the amount of Ni active sites on surface of catalysts by measuring the CO responses upon passing with injection of pure CO gas through the catalyst at room temperature. It was generally accepted that CO gas adsorbs on nickel in molecular form at room temperature. The

adsorption was possibly accompanied by formation of $Ni(CO)_4$ at low temperature and dissociation and disproportionation of CO gas at high temperature [39]. The response of curve areas corresponded to the uptake of CO molecule on the catalyst. There is an assumption that one CO molecule chemisorbed on each active Ni atom on surface[46]. Numbers of Ni atoms on the Ni catalysts surface derived from CO uptake are shown in Table 4.4 and were ranged between 16.12 - 37.89 $x10^{18}$ molecules CO/g.cat: imp_Ni-K/Al_2O_3> imp_Ni-Mn/Al_2O_3 > imp_Ni-La/Al_2O_3 > imp_Ni-Ce/Al_2O_3 > imp_Ni/Al_2O_3 ≈ imp_Ni-Mg/Al_2O_3 respectively. The promoted Ni/Al_2O_3 catalyst with K promoter displayed the highest CO chemisorption $37.89x10^{18}$ molecules CO/g.cat, resulting in the best dispersion of metal on support at 1.85% in this study. The existence of promoter in Ni/Al_2O_3 led to the increase of active Ni atoms on the catalyst surface.

Table 4.4 CO chemisorption of non-promoted and promoted nickel catalysts.

Catalyst	**CO Chemisorption Results**	
	CO chemisorption ($\times10^{-18}$ molecules/g.cat)	% Dispersion
imp_Ni/Al_2O_3	16.91	0.82
imp_Ni-Ce/Al_2O_3	20.69	1.01
imp_Ni-K/Al_2O_3	37.89	1.85
imp_Ni-La/Al_2O_3	23.46	1.14
imp_Ni-Mg/Al_2O_3	16.12	0.79
imp_Ni-Mn/Al_2O_3	27.59	1.34

จุฬาลงกรณ์มหาวิทยาลัย
Chulalongkorn University

4.1.2 The catalytic performance of the Ni/Al_2O_3 catalysts in carbon dioxide hydrogenation.

The catalytic performances of catalysts in CO_2 hydrogenation at 500 °C in terms of the conversion of CO_2 and CH_4 selectivity are shown in Table 4.5 and Figure 4.4. The CO_2 conversions of all the Ni-based catalysts were ranged between 61.30 - 82.03% and CH_4 selectivity of all catalysts were approximately 100% at steady state. The promoted Ni showed higher CO_2 conversion than the non-promoted Ni catalysts. The order of conversion was imp_Ni-K/Al_2O_3 > imp_Ni-Mn/Al_2O_3 > imp_Ni-La/Al_2O_3 > imp_Ni-Ce/Al_2O_3 > imp_Ni-Mg/Al_2O_3 > imp_Ni/Al_2O_3. The H_2-TPR and CO chemisorption characterization show that the reducibility, %dispersion and the number of nickel active sites of Ni/Al_2O_3 catalysts increased with the addition of K, Mn, La, and Ce. The reduction temperatures of β-type NiO species of imp_Ni-K/Al_2O_3, imp_Ni-Mn/Al_2O_3, imp_Ni-La/Al_2O_3, and imp_Ni-Ce/Al_2O_3 also shifted to lower temperature led to the generated active nickel (Ni^0) on the catalyst surface more than the non-promoted catalyst at low temperature. The Ni/Al_2O_3 promoted with K showed the best catalytic performances according to the aforementioned characterizations. There were also the corresponding SEM and XRD that K promoter had smaller NiO crystallite size. Thus, it is resulted in the higher dispersion of nickel species on surface and lower agglomeration of catalysts.

Adding Mg with Ni/Al_2O_3 catalysts had the tendency to increase β2-type and γ-type NiO specie, which was a strong Ni–Al interaction so that the reducibility at low temperature decreased. However, the H_2 consumption from H_2-TPR characterization, determined by reducing from room temperature to 800 °C with H_2 gas, showed the higher quantity of H_2 consumption than the non-promoted catalyst. In this study, using reduction temperature at 400 °C for 4 h had enough capability to form active Ni^0 species which made imp_Ni-Mg/Al_2O_3 more active than imp_Ni/Al_2O_3 catalysts in CO_2 hydrogenation.

Table 4.5 The CO_2 conversion and product selectivity during CO_2 hydrogenation of nickel catalysts.

Sample	CO_2 Conversion[a] (%)	CH_4 Selectivity[a] (%)	
		CH_4	CO
imp_Ni/Al_2O_3	61.30	98.83	1.17
imp_Ni-Ce/Al_2O_3	77.22	100.00	0.00
imp_Ni-K/Al_2O_3	82.03	100.00	0.00
imp_Ni-La/Al_2O_3	78.99	100.00	0.00
imp_Ni-Mg/Al_2O_3	73.56	98.94	1.06
imp_Ni-Mn/Al_2O_3	79.70	99.13	0.87

[a] At 5 h of reaction

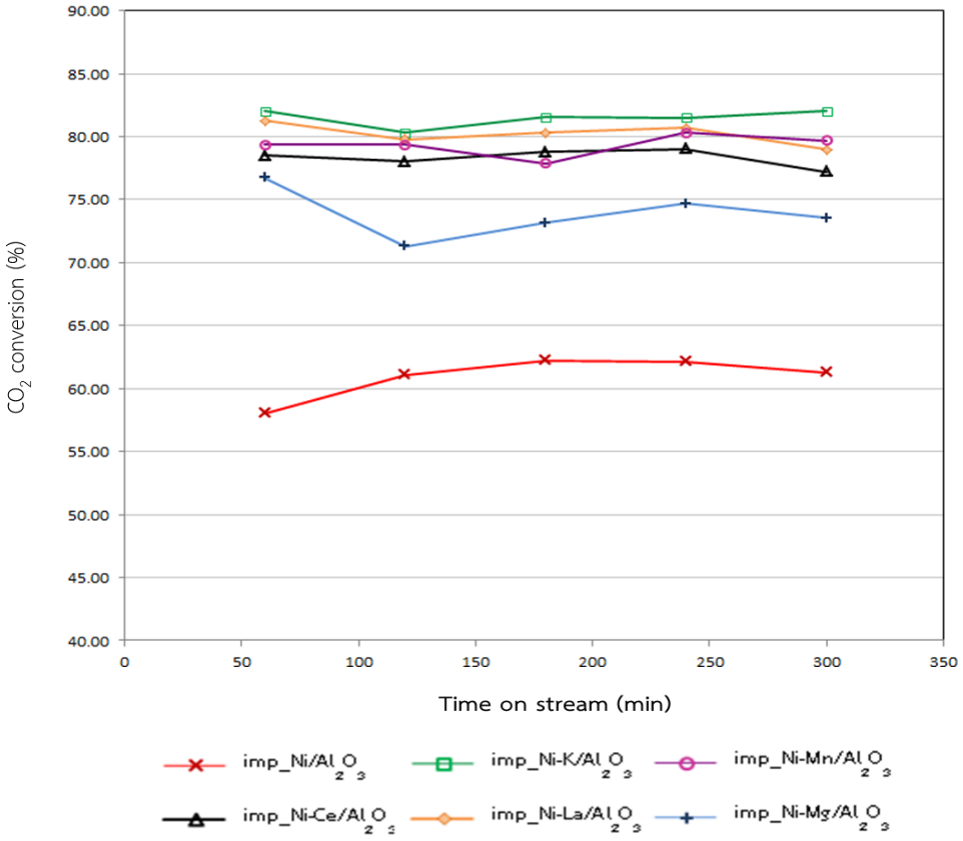

Figure 4.4 The catalytic activities of the Ni/Al_2O_3 catalysts in CO_2 hydrogenation.

4.2 Effect of K and Ce promoters on the Ni/Al_2O_3 catalysts prepared by solid-state reaction with and without dry ball mill and compare to the conventional impregnation method.

The catalyst nomenclatures are as shown below:

imp_Ni/Al_2O_3 presents the catalyst which was prepared from the mixture of nickel nitrate and gibbsite by incipient wetness impregnation

imp_Ni-Ce/Al_2O_3 presents the catalyst which was prepared from the mixture of nickel nitrate, cerium nitrate and gibbsite by incipient wetness impregnation

imp_Ni-K/Al_2O_3 presents the catalyst which was prepared from the mixture of nickel nitrate, potassium nitrate and gibbsite by incipient wetness impregnation

ss_Ni/Al_2O_3 presents the catalyst which was prepared from the mixture of nickel nitrate and gibbsite by solid-state reaction without dry ball mill calcined at 500°C.

ss_Ni-Ce/Al_2O_3 presents the catalyst which was prepared from the mixture of nickel nitrate, cerium nitrate and gibbsite by solid-state reaction without dry ball mill calcined at 500°C.

ss_Ni-K/Al_2O_3 presents the catalyst which was prepared from the mixture of nickel nitrate, potassium nitrate and gibbsite by solid-state reaction without dry ball mill calcined at 500°C

bm_Ni/Al_2O_3_12h presents the catalyst which was prepared from the mixture of nickel nitrate and gibbsite by solid-state reaction with dry ball mill using milling time 12 h calcined at 500°C.

bm_Ni/Al_2O_3_24h presents the catalyst which was prepared from the mixture of nickel nitrate and gibbsite by solid-state reaction with dry ball mill using milling time 24 h calcined at 500°C.

bm_Ni-Ce/Al_2O_3_12h presents the catalyst which was prepared from the mixture of nickel nitrate, cerium nitrate and gibbsite by solid-state reaction with dry ball mill using milling time 12 h calcined at 500°C.

Bm_Ni-K/Al_2O_3 presents the catalyst which was prepared from the mixture of nickel nitrate, potassium nitrate and gibbsite by solid-state reaction with dry ball mill using milling time 12 h calcined at 500°C.

4.2.1 Catalysts characterization

4.2.1.1 X-ray diffraction (XRD)

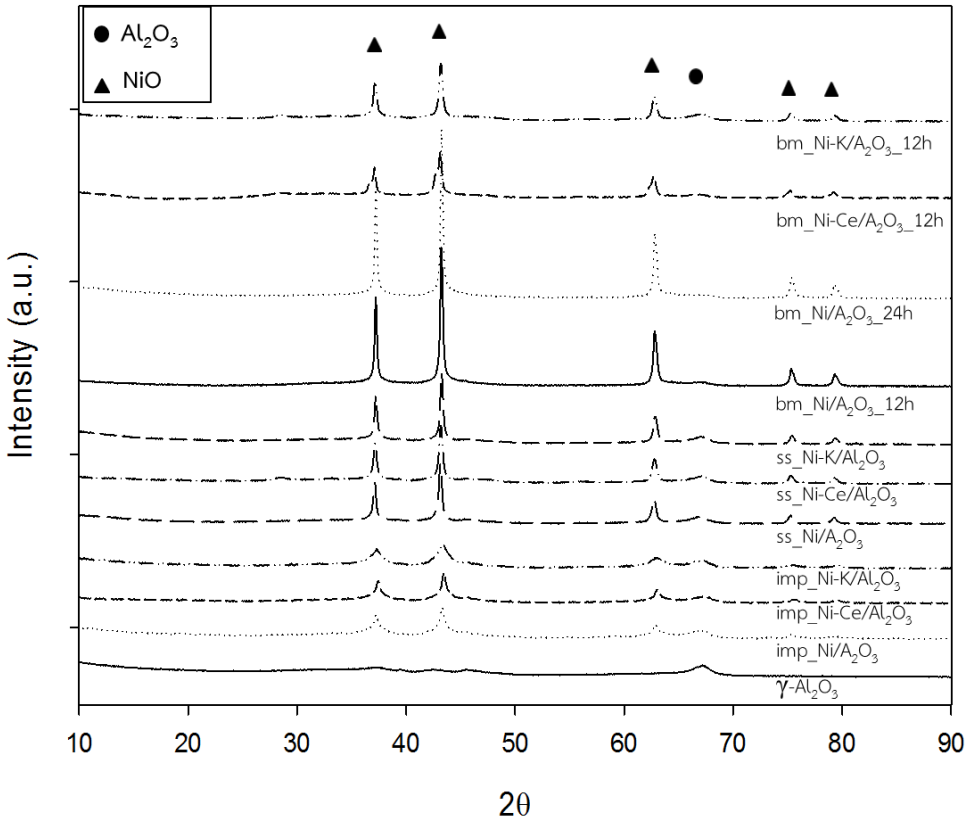

Figure 4.5 The XRD patterns of support and Ni/Al_2O_3 catalysts with Ce, K promoters prepared by the solid-state reaction with and without dry ball including the incipient wetness impregnation

The XRD patterns of Ni/Al_2O_3 catalysts with K and Ce promoters which were prepared by the solid-state reaction with and without dry ball including the incipient wetness impregnation are shown in Figure 4.5. The scanning of XRD peak in the 2θ range of 10-90° indicates 2θ degrees = 37.3°, 43.3°, 62.9°, 75.3°, and 79.5° (JCPDS 47-1049).These could be assigned to NiO because their peak positions were almost identical. In all catalysts, there were peaks 2θ = 67.0° (JCPDS 10-0425) corresponding γ-Al_2O_3. In the XRD patterns of support, small peaks were found around 2θ = 43°, where a small amount of χ-phase crystalline occurred in alumina support. For the promoted catalysts, the XRD peaks corresponding to K and Ce species were not detected because they were smaller than the detection limit of the XRD or due to the very small amount present. For the non-promoted Ni/Al_2O_3 that was prepared by the solid-state reaction, higher intensities of the NiO peaks were seen compared to the non-promoted Ni/Al_2O_3, prepared by impregnation. In addition, the solid-state with ball mill showed higher intensity than that without ball mill. When using the same method for preparation, adding K and Ce in Ni/Al_2O_3 catalysts showed lower and wider intensity of the NiO peaks than non-promoted Ni/Al_2O_3.

The NiO crystallite sizes of all Ni-based catalysts were ranged between 6.5 to 33.0 nm and were categorized in nanometer range as shown in Table 4.6. The preparation of Ni/Al_2O_3 promoted with K by incipient wetness impregnation resulted in relatively low intensity and broader peaks. Such results suggest that the crystallite size of NiO particles may be very small (6.5 nm) compared to the other catalysts in this study. Average crystallite sizes of NiO of Ni/Al_2O_3 catalysts prepared by solid state without dry ball mill were in the order; ss_Ni/Al_2O_3 > ss_Ni-Ce/Al_2O_3 > ss_Ni-K/Al_2O_3. The average crystallite sizes of NiO particles of non-promoted catalysts obtained from the solid-state reaction with dry ball mill using milling time 24h was 33 nm which was larger than milling time 12 h (27 nm). When adding Ce and K on Ni/Al_2O_3 with milling time of 12h, the NiO crystallite sizes were reduced to 13.2 and 19.9 nm respectively. Adding K, Ce promoter on Ni/Al_2O_3 in all preparation method made average crystallite sizes of NiO reduced indicating the well dispersed of NiO over the supports.

จุฬาลงกรณ์มหาวิทยาลัย
CHULALONGKORN UNIVERSITY

Table 4.6 Average NiO crystallite size of Ni-based catalysts with Ce, K promoters prepared by the solid-state reaction with and without dry ball including the incipient wetness impregnation

Sample	Average NiO crystallite size from XRD (nm)
imp_Ni/Al_2O_3	14.8
imp_Ni-Ce/Al_2O_3	14.1
imp_Ni-K/Al_2O_3	6.5
ss_Ni/Al_2O_3	22.7
ss_Ni-Ce/Al_2O_3	19.9
ss_Ni-K/Al_2O_3	17.6
bm_Ni/Al_2O_3_12h	27.4
bm_Ni/Al2O3_24h	33.0
bm_Ni-Ce/Al_2O_3_12h	13.2
bm_Ni-K/Al_2O_3_12h	19.9

จุฬาลงกรณ์มหาวิทยาลัย
Chulalongkorn University

4.1.1.2 Nitrogen physisorption

Nitrogen physisorption was used to examine textural properties of supports and catalysts. The BET surface area, pore volume and average pore size diameters of all the catalysts samples are summarized in Table 4.7. Pure γ-Al_2O_3 support had the surface area of 162.7 m^2/g. The BET surface areas and pore volume of the catalysts prepared by the solid-state were ranged between 130.8–149.6 m^2/g and 0.17–0.24 cm^3/g, whereas the catalysts prepared by impregnation were ranged between 93.0–108.5 m^2/g and 0.13–0.16 cm^3/g. The BET surface area and pore volume of the

catalyst prepared by the incipient wetness impregnation decreased. It is suggested that nickel nitrate precursor solutions were adsorbed deeply in the pores of the gamma alumina support, as the result; there was the formation of nickel oxide particles inside the pores. When prepared by solid-state reaction, most of the nickel oxide particles appeared to be deposited on the external surface of the alumina supports.

Table 4.7 Physiochemical of Ni-based catalysts with Ce, K promoters prepared by the solid-state reaction with and without dry ball including the incipient wetness impregnation

Sample	BET surface area (m^2 / g)	Average pore volume (cm^3/g)	Average pore size (nm)
γ-Al_2O_3	162.7	0.21	3.25
imp_Ni/Al_2O_3	103.1	0.15	3.5
Imp_Ni-Ce/Al_2O_3	108.5	0.16	3.44
imp_Ni-K/Al_2O_3	93.0	0.13	3.5
ss_Ni/Al_2O_3	149.6	0.24	4.1
ss_Ni-Ce/Al_2O_3	144.5	0.20	3.72
ss_Ni-K/Al_2O_3	141.3	0.19	3.77
bm_Ni/Al_2O_3_12h	134.6	0.19	3.80
bm_Ni/Al_2O_3_24h	130.8	0.17	3.84
bm_Ni-Ce/Al_2O_3_12h	136.7	0.19	3.98
bm_Ni-K/Al_2O_3_12h	134.2	0.19	4.01

จุฬาลงกรณ์มหาวิทยาลัย
Chulalongkorn University

4.2.1.3 Hydrogen temperature program reduction (H_2-TPR)

The H_2-TPR profile of Ni-based catalysts prepared by solid-state reaction and the incipient wetness impregnation are shown in Figure 4.6. Metal-support interaction leads to different reduction behaviors and reducibility of nickel species on the support. The reducible NiO species could be classified into four types: α-type (NiO species can be either free nickel oxide or bulk NiO or weakly interact with alumina support) by the show reduction peak at 180-260°C. β_1-type (NiO species that are weakly interacted with Al_2O_3 or called Ni-rich mixed oxide phase) and β_2-type (NiO species that are weakly interacted with Al_2O_3 or called Al-rich phase) where indicated at the reduction peaks around 260-500°C. γ-type (NiO species strongly interact with the support, which in this study are shown by the reduction peak around 500-840°C . It is difficult to reduce a stable nickel aluminate phase or $NiAl_2O_4$ to Ni^0 species at low temperature.

For the Ni/Al_2O_3 catalysts prepared by the solid-state reaction, the reduction peak indicated that most of NiO species was β-type. The Ni/Al_2O_3 catalysts prepared by the solid-state reaction with ball mill showed significantly higher area peak of β-NiO species peak than the Ni/Al_2O_3 catalysts prepared by the solid-state reaction without dry ball mill. The Ni/Al_2O_3 catalysts prepared by incipient wetness impregnation showed the reduction peak located in γ-NiO species more than solid-state reaction. It suggests that catalysts that were prepared by incipient wetness impregnation had smaller sizes of NiO, they were better dispersed on the catalyst surface[1]. This corresponded to smaller NiO crystallite sizes calculated from the XRD.

The amounts of H_2 consumed /g cat were calculated from the H_2-TPR results and are summarized in Table 4.8. H_2 consumed were found to be in the order as followed: bm_Ni-K/Al_2O_3_12h > bm_Ni-Ce/Al_2O_3_12h≈ bm_Ni/Al_2O_3_24h > bm_Ni/Al_2O_3 _12h> imp_ Ni-K/Al_2O_3 > imp_Ni-Ce/Al_2O_3 > imp_ Ni/Al_2O_3 > ss_Ni-K/ Ni/Al_2O_3 > ss_Ni-Ce/Al_2O_3 > ss_ Ni/Al_2O_3. The amount of H_2 consumption of the Ni/Al_2O_3 prepared by solid-state reaction with dry ball mill was more than

impregnation and solid-state reaction without dry ball mill. When using the same preparation method, the promoted Ni catalysts had higher H_2 consumption than the non-promoted ones.

Table 4.8 H_2 consumption of Ni-based catalysts with Ce, K promoters prepared by the solid-state reaction and the incipient wetness impregnation

Sample	H_2 consumption (umol/g)
imp_Ni/Al_2O_3	19550
imp-Ni-Ce/Al_2O_3	19837
imp_Ni-K/Al_2O_3	22397
ss_Ni/Al_2O_3	16965
ss_Ni-Ce/Al_2O_3	17393
ss_Ni-K/Al_2O_3	17506
bm_Ni/Al_2O_3_12h	31094
bm_Ni/Al_2O_3_24h	32343
bm_Ni-Ce/Al_2O_3_12h	32354
bm_Ni-K/Al_2O_3_12h	33287

จุฬาลงกรณ์มหาวิทยาลัย
Chulalongkorn University

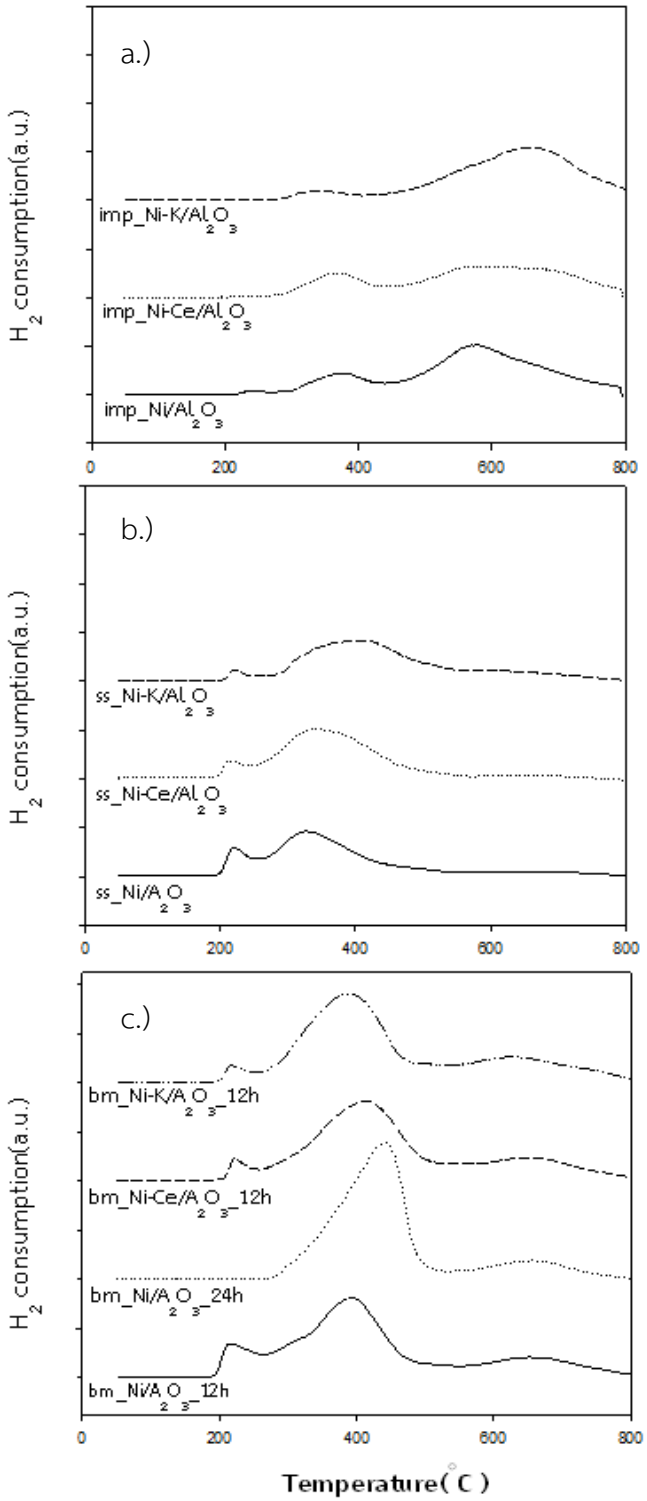

Figure 4.6 The TPR profiles of Ni/Al_2O_3 catalysts with Ce, K promoter prepared by a.) impregnation, b.) solid-state reaction without dry ball mill and c.) solid-state reaction with dry ball mill

4.2.1.4 Scanning electron microscopy analyses (SEM)

The SEM images of Ni/Al_2O_3 catalysts with Ce, K promoters prepared by impregnation and solid-state method are shown in Figure 4.7. All the prepared nickel catalysts showed the same morphology that were non-uniform particle sizes and shapes. However, there were little differences in terms of the agglomeration of primary particles due to the addition K, Ce promoters and methods of catalyst preparation. It is noticeable on SEM images that nickel catalysts prepared by solid-state displayed smaller particle sizes than those prepared by impregnation method. For nickel catalysts prepared by impregnation, the K promoter resulted in the decrease in agglomeration of the primary particles. But the effect of Ce and K promoters seems to show no effects in Ni/Al_2O_3 catalysts prepared by the solid-state method.

จุฬาลงกรณ์มหาวิทยาลัย
Chulalongkorn University

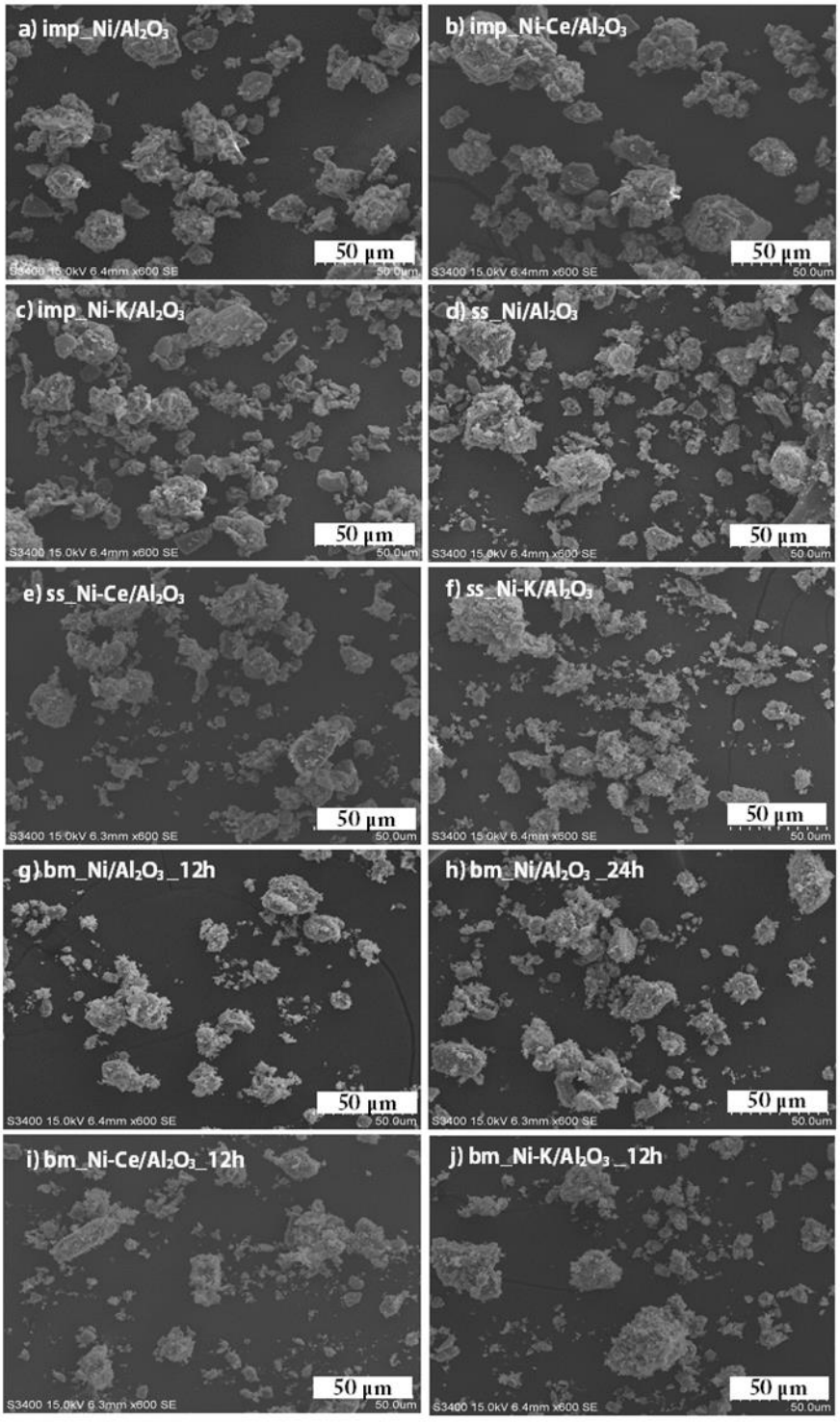

Figure 4.7 The SEM images of $Ni/A_{l2}O_3$ catalysts with Ce, K promoter prepared by impregnation, solid-state reaction without dry ball mill and solid-state with dry ball mill.

4.2.1.5 Carbon mono oxide chemisorption

Numbers of Ni atoms on the Ni catalysts prepared by solid-state and impregnation method were derived from CO uptake, and are shown in Table 4.9. The Ni active sites were ranged between 12.16 - 37.89 x10^{18} molecules CO/g.cat. The order of Ni active sites was Ni-K/Al_2O_3 > bm_Ni-Ce/Al_2O_3_12h > Ni-Ce/Al_2O_3 Ni/Al_2O_3 > ss_Ni-K/Al_2O_3 > ss_Ni-Ce/Al_2O_3 > bm_Ni-K/Al_2O_3_12h> bm_Ni/Al_2O_3_12h > bm_Ni/Al_2O_3_24h > ss_Ni/Al_2O_3respectively. Percent dispersion was calculated by the amount of Ni active sites per Ni loading of Ni/Al_2O_3.

The Ni-based catalysts which were prepared by the incipient wetness impregnations gave higher %dispersion than the solid-state reaction. Adding Ce and K promoter on Ni/Al_2O_3 catalyst led to higher %dispersion and Ni active sites. The efficiency of promoters was different when using different preparing methods. The Ni/Al_2O_3 catalyst with K promoter prepared by impregnation method showed the highest CO chemisorption at 37.89x10^{18} molecules CO/g.cat and the best %dispersion of metal on support at 1.85% in this study. Secondly, the bm_Ni-Ce/Al_2O_3 had the chemisorption 22.53 x 10^{18} molecules CO/g.cat and %dispersion of metal on support 1.04 %. The Ce promoter showed higher Ni active sites when prepared by solid state with ball mill which was higher than the Ni-Ce/Al_2O_3 that was prepared by impregnation and solid state without ball mill.

Table 4.9 CO chemisorption of Ni-based catalysts with Ce, K promoters prepared by the solid-state reaction with and without dry ball including the incipient wetness impregnation

Sample	CO chemisorption ($\times 10^{-18}$ molecules/g.cat)	% Dispersion
imp_Ni/Al_2O_3	16.91	0.82
imp_Ni-Ce/Al_2O_3	20.69	1.01
imp_Ni-K/Al_2O_3	37.89	1.85
ss_Ni/Al_2O_3	12.38	0.60
ss_Ni-Ce/Al_2O_3	17.16	0.84
ss_Ni-K/Al_2O_3	17.59	0.86
bm_Ni/Al_2O_3_12h	13.63	0.66
bm_Ni/Al_2O_3_24h	13.38	0.64
bm_Ni-Ce/Al_2O_3_12h	22.53	1.04
bm_Ni-K/Al_2O_3_12h	15.93	0.76

จุฬาลงกรณ์มหาวิทยาลัย
Chulalongkorn University

4.2.1.6 X-ray photoelectron spectroscopy (XPS)

Nickel species and the relative quantity of element on the surface of catalysts were studied by XPS characterization. The catalysts were investigated in the Ni 2p, Ce 3d, K 1s, Al 2p, O 1s, C 1s binding energy regions. XPS spectra of Ni species on the catalysts surface in this study was related to a previous research [47]. The XPS spectra of Ni species on the catalysts surface showed in Figure 4.8. It exists of the peaks of Ni $2p_{3/2}$ and Ni $2p_{1/2}$ core levels, which were displayed centered at around 855.51 and 873.01 respectively. XPS spectra specific to Ni $2p_{3/2}$ of the catalysts have

two types of Ni species corresponding to the main peaks at around 854 and 860 eV, respectively [2]. According to the H_2-TPR results, it could be inferred that the two Ni species might be NiO (weak interactions with the support) and $NiAl_2O_4$ (strong interactions with the support) on the catalyst surfaces [27].

Table 4.10 The binding energy, FWHM of Ni $2p_{3/2}$ and the ratio of percentages of atomic concentration of the nickel catalysts

Sample	Ni (II) 2p3/2		Atomic Conc %			
	B.E. (eV)	FWHM	Ce/Ni	K/Ni	Ni/Al	Al/O
imp_Ni/Al_2O_3	856	4.485	0	0	0.454	0.687
imp_Ni-Ce/Al_2O_3	855.1	4.542	0.067	0	0.494	0.599
imp_Ni-K/Al_2O_3	856.5	4.218	0	0.073	0.305	0.410
ss_Ni/Al_2O_3	857.2	4.944	0	0	0.676	0.696
ss_Ni-Ce/Al_2O_3	856.1	4.631	0.038	0	0.682	0.721
ss_Ni-K/Al_2O_3	855.7	4.047	0	0.012	0.443	0.930
bm_Ni/Al_2O_3_12h	856.5	4.126	0	0	0.680	0.471
bm_Ni/Al_2O_3_24h	855.3	4.056	0	0	0.693	0.704
bm_Ni-Ce/Al_2O_3_12h	858	4.433	0.024	0	0.766	0.572
bm_Ni-K/Al_2O_3_12h	856	3.774	0	0.013	0.718	0.517

The binding energy, FWHM of Ni $2p_{3/2,}$ and the ratios of percentages of atomic concentration are summarized in Table 4.10. The Ni/Al atomic concentration of the Ni catalysts prepared by the solid-state reaction was more than Ni catalysts prepared by the incipient wetness impregnation. It was found that the Ni-based catalysts prepared by the incipient wetness impregnation showed lower the amount of nickel

on surface. The results were in corresponding to the BET surface area and pore volume results that displayed the Ni-based catalysts prepared by solid-state reaction had more amounts of nickel oxide particles being deposited on the external surface of the alumina supports than the prepared Ni-based catalysts by the incipient wetness impregnation.

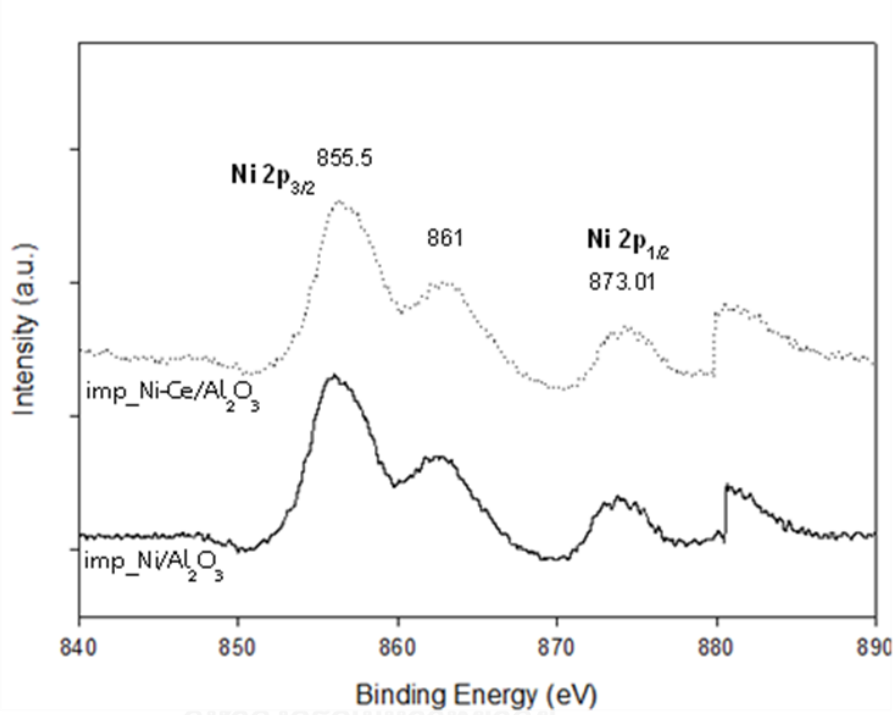

Figure 4.8 XPS energy spectrum for Ni 2p levels in of the sample of nickel catalysts.

.

4.2.1.6 Particle size analysis

The particle sizes of Ni/Al_2O_3 catalysts with K and Ce promoters which were prepared by the solid-state reaction with and without dry ball including the incipient wetness impregnation were analyzed by a Zetasizer with nano series model from Malvern Instruments Ltd. Dynamic Light Scattering (DLS) is an important tool for analysis the size of nanoparticles in solution. In an unagglomerated suspension, the DLS measured diameter will be similar or quite larger than the TEM size. The DLS

measurement was always much larger than the TEM size and can have a high polydispersity index (large variability in the particle size when particles were agglomerated.

The particle sizes of the Ni/Al_2O_3 catalysts are summarized in Table 4.11. The radius of the catalysts was ranged between 582-143 nm. Particle sizes of Ni/Al_2O_3 catalysts prepared by sold-state reaction were smaller than the Ni/Al_2O_3 catalysts prepared by impregnation method. Solid-state reaction method with dry ball mill made slightly smaller particle sizes of the Ni/Al_2O_3 catalysts than using sold-state reaction without dry ball mill. Using ball mill in preparation process, may lead to a well-mixed catalysts and the reduction of particle sizes.

Table 4.11 Particle size of of Ni-based catalysts with Ce, K promoters prepared by the solid-state reaction with and without dry ball including the incipient wetness impregnation

Sample	Radius (nm)	Pdl
imp_Ni/Al_2O_3	582	0.67
imp_$Ni\text{-}Ce/Al_2O_3$	469	0.62
imp_$Ni\text{-}K/Al_2O_3$	554	0.29
ss_Ni/Al_2O_3	350	0.38
ss_$Ni\text{-}Ce/Al_2O_3$	172	0.38
ss_$Ni\text{-}K/Al_2O_3$	280	0.43
bm_Ni/Al_2O_3_12h	316	0.30
bm_Ni/Al_2O_3_24h	319	0.28
bm_$Ni\text{-}Ce/Al_2O_3$_12h	143	0.34
bm_$Ni\text{-}K/Al_2O_3$_12h	209	0.44

จุฬาลงกรณ์มหาวิทยาลัย
Chulalongkorn University

4.2.2 The catalytic performance of the Ni/Al_2O_3 catalysts in carbon dioxide hydrogenation

The Ni/Al_2O_3 catalysts with K and Ce promoters prepared by the solid-state reaction with and without dry ball mill and the incipient wetness impregnation were tested in CO_2 hydrogenation at 500 ºC and 1 atm total pressure.

Catalytic performances determined from the conversion of CO_2 and CH_4 selectivity are shown in Table 4.12, Figure 4.9 and Figure 4.10. The CO_2 conversions of all the Ni-based catalysts at steady state were ranged between 56.30 - 82.03% and CH_4 selectivity of all catalysts were approximately 100% at steady state. Conversion of all catalysts at steady state can be ranked in the order: imp_Ni-K/Al_2O_3 > bm_Ni-Ce/Al_2O_3_12h> imp_Ni-Ce/Al_2O_3 > ss_Ni-K/Al_2O_3 > bm_Ni-K/Al_2O_3 > ss_Ni-Ce/Al_2O_3 > bm_Ni/Al_2O_3_12h > bm_Ni/Al_2O_3_24h >imp_Ni/Al_2O_3 > ss_Ni/Al_2O_3 respectively. Promoted Ni/Al_2O_3 prepared by both solid-state reaction and the incipient wetness impregnation gave higher CO_2 conversion than non-promoted Ni catalysts. According to the characterization used in this study, it is shown that K, Ce promoter can improve catalytic properties of the non-Ni/Al_2O_3 catalyst.

The CO_2 conversion of the non-promoted Ni/Al_2O_3 catalysts was in the order: bm_Ni/Al_2O_3_12h >bm_Ni/Al_2O_3_24h > imp_Ni/Al_2O_3 > ss_Ni/Al_2O_3. The non-promoted Ni/Al_2O_3 prepared by solid-state reaction without dry ball mill exhibited slightly lower CO_2 conversion than the ones prepared by impregnating method. According to the CO chemisorption results, the amounts of nickel active sites of ss_Ni/Al_2O_3 were lower than Ni/Al_2O_3 catalysts prepared by incipient wetness impregnation. Using dry ball mill in preparation process of Ni-based catalysts with solid-state reaction can increase CO_2 conversion. This is because of high amount of NiO species on the surface as characterized by H_2-TPR, N_2 physisorption, and XPS. From the performances and characterization of the catalysts prepared by the solid-state reaction with dry ball mill, it is indicated that 12 h milling time was better than 24 h. When comparing performance of the non-promoted catalysts between preparing catalysts via solid-state reaction with dry ball mill and impregnation, both

bm_Ni/Al_2O_3_12h and bm_Ni/Al_2O_3_24h gave higher CO_2 conversion than the imp_Ni/Al_2O_3. The main characteristics differences between the solid-state and the impregnation method were probably the NiO particle size and the location of Ni particles on the gamma alumina support. From the N_2 physisorption and XPS analyses, many NiO particles/granules were located inside the pores of the alumina supports when prepared by impregnation. In contrast, the solid-state reaction resulted in NiO particles located on the external surface of the support of catalysts. The impregnation preparation gave the average crystallite size of NiO much smaller than those obtained from the solid-state reaction. For CO_2 hydrogenation over nickel catalysts, it has been proven that the reaction between CO_2 molecules and active nickle species moved via CO_2 dissociation to adsorbed CO and O on the catalyst surface and reverse water–gas shift reaction[16]. At the time when the surface of the catalysts was controlled by the strong adsorption of CO, the diffusion of CO_2 molecules in the pores of alumina was retarded. In this case, the reaction of CO_2 on some of the active Ni species located deeply inside the pores of alumina. It is resulting in the slow CO_2 adsorption and dissociation to adsorbed CO and O on the Ni metal surface. From these reasons, it is likely that the non-promoted Ni/Al_2O_3 obtained via the solid-state reaction with dry ball milling, exhibited better catalytic performances in the CO_2 hydrogenation reaction than those prepared by impregnation, although the CO chemisorption showed that both bm_Ni/Al_2O_3_12h and bm_Ni/Al_2O_3_24h had slightly smaller amount of Ni active sites than the imp_Ni/Al_2O_3.

However, the Ni/Al_2O_3 promoted with K prepared by impregnation led to the best catalytic performance due to the highest metal dispersion according to the aforementioned characterizations. There were also the corresponding SEM and XRD that K promoter resulted in smaller NiO crystallite sizes which were easier to reduce to active nickel. Although some active sites were in the pores, they still showed the highest conversion at 82.03% and selectivity at 100% at steady state.

The next rank of conversion with a small difference from the catalysts with the highest conversion was the bm_Ni-Ce/Al_2O_3. It had CO_2 conversion as 81.16% and

CH_4 selectivity at 99.15%. The Ce promoter was highly efficient when using to promote Ni/Al_2O_3, prepared by solid state with ball mill than using impregnation and solid state without ball mill preparation.

Table 4.12 The CO_2 conversion and product selectivity during CO_2 hydrogenation of nickel catalysts.

Sample	CO_2 Conversion[a] (%)	Product selectivity[a] (%)	
		CH_4	CO
imp_Ni/Al_2O_3	61.30	98.83	1.17
imp_$Ni\text{-}Ce/Al_2O_3$	77.22	100.00	0.00
imp_$Ni\text{-}K/Al_2O_3$	82.03	100.00	0.00
ss_Ni/Al_2O_3	56.30	97.23	2.77
ss_$Ni\text{-}Ce/Al_2O_3$	73.73	98.82	1.18
ss_$Ni\text{-}K/Al_2O_3$	76.30	98.25	1.75
bm_Ni/Al_2O_3_12hr	71.57	98.63	1.37
bm_Ni/Al_2O_3_24hr	69.28	97.63	2.37
bm_$Ni\text{-}Ce/Al_2O_3$_12hr	81.16	99.15	0.85
bm_$Ni\text{-}K/Al_2O_3$_12hr	74.22	98.84	1.16

[a] At 5 h of reaction.

จุฬาลงกรณ์มหาวิทยาลัย
Chulalongkorn University

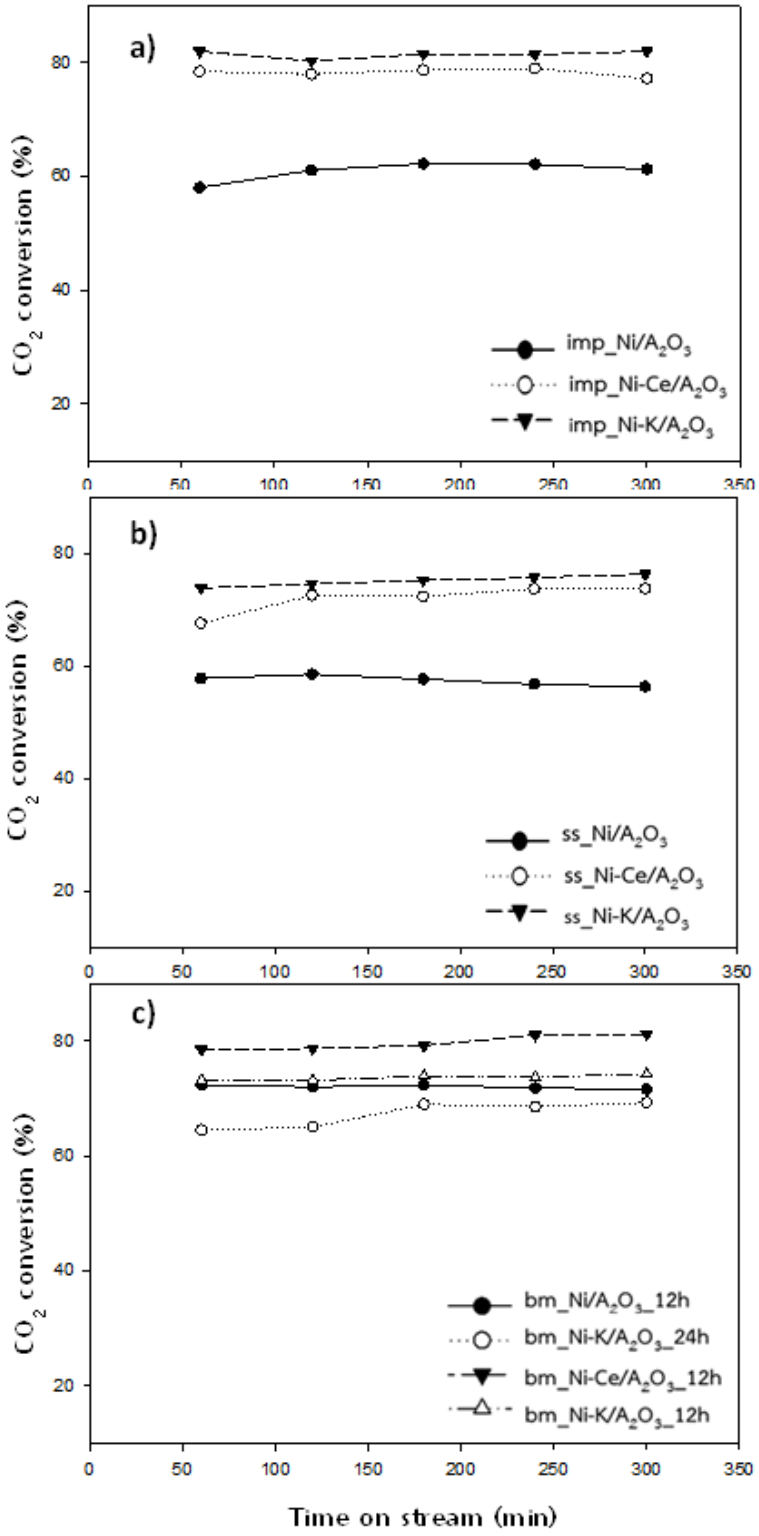

Figure 4.9 The catalytic activities in carbon dioxide hydrogenation of Ni/Al_2O_3 catalysts with Ce, K promoter prepared a.) impregnation, b.) solid-state reaction without dry ball mill and c.) solid-state reaction with dry ball mill

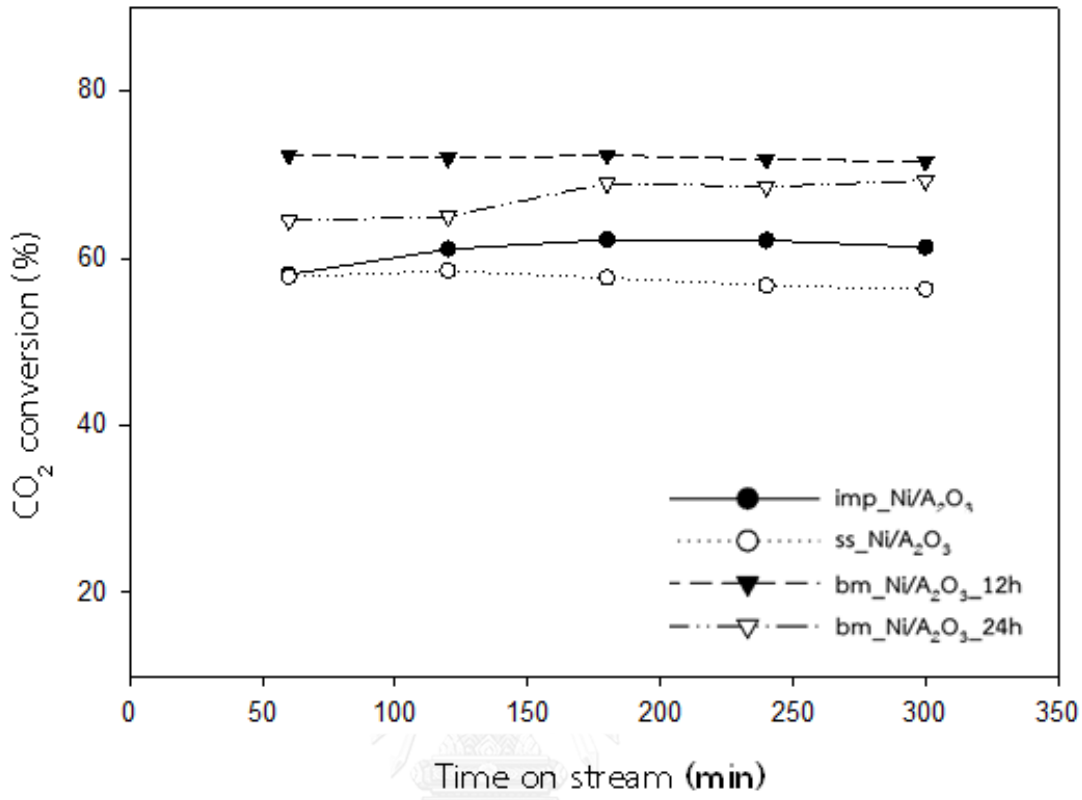

Figure 4.10 The catalytic activities in carbon dioxide hydrogenation of non-promoted Ni/Al_2O_3 catalysts prepared by the solid-state reaction with and without dry ball mill and the incipient wetness impregnation

จุฬาลงกรณ์มหาวิทยาลัย
Chulalongkorn University

CHAPTER V
CONCLUSIONS AND RECOMMENDATIONS

5.1 Conclusions

In this study, the effects of different types of promoter (K, Mn, La, Ce, and Mg) on the physiochemical and catalytic properties of modified Ni/Al_2O_3 catalysts prepared by incipient wetness impregnation were investigated. Among all promoters, Ce and K were selected to continue the study of the effect of catalyst preparation including solid-state reaction with and without milling process and the results were compared to those obtained by the conventional impregnation method. The results can be concluded as followed:

1) In the case of impregnation-made catalysts, Ni/Al_2O_3 catalysts promoted with potassium, manganese, lanthanum, cerium, and magnesium were studied for CO_2 hydrogenation reaction at 500 °C. Potassium was found to be the best promoter which gave the highest CO conversion at 82.03% and CH_4 selectivity at 100%. The imp_Ni-K/Al_2O_3 catalyst exhibited the highest reducibility, smallest NiO crystallite size, highest amount of active nickel species on the catalyst surface and the weaker metal-support interaction. Moreover, the agglomeration of nickel species on the surface of the catalysts also decreased.

2) Comparing with the conventional impregnation-made catalyst, the solid-state reaction Ni/Al_2O_3 catalysts had lower amounts of Ni active sites and exhibited lower CO_2 conversion. However after the milling process, the CO_2 conversion of solid-state reaction–made Ni/Al_2O_3 catalysts was significantly improved. Addition with Ce and K also improved the Ni dispersion and CO_2 conversion. In this case bm_Ni-Ce/Al_2O_3 exhibited the highest CO_2 conversion at 81.16 % and 100% CH_4 selectivity. The main different characteristics differences between the solid-state reaction and the impregnation method were probably the Ni particle size and the location of Ni particles on the gamma alumina support.

5.2 Recommendations

1) Study the catalyst performance in different reaction temperatures that are used in CO_2 hydrogenation reaction is very interesting because the reaction temperature is a major factor of efficient performance of catalytic reaction and the obtained data can be used for study kinetic and thermodynamic.

2) The location of metal on support influences the catalytic activity, thus, this is interesting to study the location of metal on alumina by HRTEM method.

3) The promoters may be reduced with hydrogen during reduction characterization therefore it is interesting to study the effect of reduction of potassium oxides, manganese oxides, lanthanum oxides, cerium oxides or magnesium oxides by H_2-TPR techniques.

4) Ball mill has an impaction the catalysts properties and catalytic performance that are prepared by solid-state reaction so it is interesting to investigate various types of ball mill processes to improve the catalytic performances in CO_2 hydrogenation.

จุฬาลงกรณ์มหาวิทยาลัย
Chulalongkorn University

REFERENCES

[1] Hu, D., et al. Enhanced Investigation of CO Methanation over Ni/Al_2O_3 Catalysts for Synthetic Natural Gas Production. Industrial & Engineering Chemistry Research 51(13) (2012): 4875-4886.

[2] Zhang, H., Dong, Y., Fang, W., and Lian, Y. Effects of composite oxide supports on catalytic performance of Ni-based catalysts for CO methanation. Chinese Journal of Catalysis 34(2) (2013): 330-335.

[3] Wang, B., et al. Effects of MoO_3 loading and calcination temperature on the activity of the sulphur-resistant methanation catalyst MoO_3/γ-Al_2O_3. Applied Catalysis A: General 431-432 (2012): 144-150.

[4] Duret, A., Friedli, C., and Maréchal, F. Process design of Synthetic Natural Gas (SNG) production using wood gasification. Journal of Cleaner Production 13(15) (2005): 1434-1446.

[5] Hitoshi, K., Kyoko, K.B., Kiyomi, O., and Hironori, A. Effect of metal loading on CO_2 hydrogenation reactivity over Rh/SiO_2 catalysts. Applied Catalysis 197 (2000): 255–268.

[6] Beuls, A., Swalus, C., Jacquemin, M., Heyen, G., Karelovic, A., and Ruiz, P. Methanation of CO_2: Further insight into the mechanism over Rh/γ-Al_2O_3 catalyst. Applied Catalysis B: Environmental 113-114 (2012): 2-10.

[7] Lee, S.-C., et al. Promotion of hydrocarbon selectivity in CO_2 hydrogenation by Ru component. Journal of Molecular Catalysis A: Chemical 210(1-2) (2004): 131-141.

[8] Zhao, A., Ying, W., Zhang, H., Hongfang, M., and Fang, D. Ni/Al_2O_3 catalysts for syngas methanation: Effect of Mn promoter. Journal of Natural Gas Chemistry 21(2) (2012): 170-177.

จุฬาลงกรณ์มหาวิทยาลัย
CHULALONGKORN UNIVERSITY

[9] Liu, Z., Chu, B., Zhai, X., Jin, Y., and Cheng, Y. Total methanation of syngas to synthetic natural gas over Ni catalyst in a micro-channel reactor. Fuel 95 (2012): 599-605.

[10] Park, J.-N. and McFarland, E.W. A highly dispersed Pd–Mg/SiO_2 catalyst active for methanation of CO_2. Journal of Catalysis 266(1) (2009): 92-97.

[11] Cai, M., Wen, J., Chu, W., Cheng, X., and Li, Z. Methanation of carbon dioxide on Ni/ZrO_2-Al_2O_3 catalysts: Effects of ZrO_2 promoter and preparation method of novel ZrO_2-Al_2O_3 carrier. Journal of Natural Gas Chemistry 20(3) (2011): 318-324.

[12] Chen, C.S., Lin, J.H., You, J.H., and Yang, K.H. Effects of Potassium on Ni-K/Al_2O_3 Catalysts in the Synthesis of Carbon Nanofibers by Catalytic Hydrogenation of CO_2. Physical Chemistry. 114 (2010): 3773–3781.

[13] Widegren, J.A. and Finke, R.G. A review of soluble transition-metal nanoclusters as arene hydrogenation catalysts. Molecular Catalysis 191 (2003): 187–207.

[14] Cubeiro, M.L., Morales, H., Goldwasser, M.R., and Pérez-Zurita, M.J. Hydrogenation of carbon oxides over Fe/Al_2O_3 catalysts. Applied Catalysis 189 (1999): 87-97.

[15] Shen, J.G.C. and Ichikawa, M. Intrazeolite Anchoring of Co, Ru, and [Ru-Co] Carbonyl Clusters: Synthesis, Characterization, and Their Catalysis for CO Hydrogenation. Physical Chemistry. 102 (1998): 5602-5613.

[16] Srisawad, N., Chaitree, W., Mekasuwandumrong, O., Shotipruk, A., Jongsomjit, B., and Panpranot, J. CO_2 hydrogenation over Co/Al_2O_3 catalysts prepared via a solid-state reaction of fine gibbsite and cobalt precursors. Reaction Kinetics, Mechanisms and Catalysis 107(1) (2012): 179-188.

[17] Jeletic, M.S., Mock, M.T., Appel, A.M., and Linehan, J.C. A cobalt-based catalyst for the hydrogenation of CO_2 under ambient conditions. J Am Chem Soc 135(31) (2013): 11533-6.

จุฬาลงกรณ์มหาวิทยาลัย
CHULALONGKORN UNIVERSITY

[18] Luyten, L.J.M., Eck, M.v., J. v. Grondelle, and Hooff, J.H.C.v. Hydrogenation of Carbon Monoxide over Silica Supported Nickel-Copper and Ruthenium-Copper Catalysts Physical Chemistry. 82(18) (1978).

[19] Sakurai, H. and Haruta, M. Carbon dioxide and carbon monoxide hydrogenation over gold supported on titanium, iron, and zinc oxides. Applied Catalysis 127 (1995): 93-105

[20] Mekasuwandumrong, O., Tantichuwet, P., Chaisuk, C., and Praserthdam, P. Impact of concentration and Si doping on the properties and phase transformation behavior of nanocrystalline alumina prepared via solvothermal synthesis. Materials Chemistry and Physics 107(2-3) (2008): 208-214.

[21] Mekasuwandumrong, O., Wongwaranon, N., Panpranot, J., and Praserthdam, P. Effect of Ni-modified α-Al_2O_3 prepared by sol–gel and solvothermal methods on the characteristics and catalytic properties of Pd/α-Al_2O_3 catalysts. Materials Chemistry and Physics 111(2-3) (2008): 431-437.

[22] Pansanga, K., Panpranot, J., Mekasuwandumrong, O., Satayaprasert, C., Goodwin, J.G., and Praserthdam, P. Effect of mixed γ- and χ-crystalline phases in nanocrystalline Al_2O_3 on the dispersion of cobalt on Al_2O_3. Catalysis Communications 9(2) (2008): 207-212.

[23] Hwang, S., et al. Methanation of Carbon Dioxide Over Mesoporous Nickel–M–Alumina (M = Fe, Zr, Ni, Y, and Mg) Xerogel Catalysts: Effect of Second Metal. Catalysis Letters 142(7) (2012): 860-868.

[24] Nor, A.B., Wan, A.W.A.B., Faridah, M.M., and Moh, d.H.R. CO_2 / H_2 Methanatin on nickel oxide based catalayst doped with various elements for the purification of natural gas The Malaysian Journal of Analytical Sciences 12 (2008): 217-223.

[25] Li, F., Yu, X., Pan, H., Wang, M., and Xin, X. Syntheses of MO_2 (M=Si, Ce, Sn) nanoparticles by solid-state reactions at ambient temperature. Solid State Sciences 2 (2000): 767-772.

จุฬาลงกรณ์มหาวิทยาลัย
Chulalongkorn University

[26] Homs, N., Toyir, J., and de la Piscina, P.R. Catalytic Processes for Activation of CO_2. (2013): 1-26.

[27] Trimm, D.L. Dwsign of Industrial Catalysts. Amsterdam Oxfod New York Elsevier scientific Publishing Company, 1980.

[28] Prasad Yadav, T., Manohar Yadav, R., and Pratap Singh, D. Mechanical Milling: a Top Down Approach for the Synthesis of Nanomaterials and Nanocomposites. Nanoscience and Nanotechnology 2(3) (2012): 22-48.

[29] Inthawong, S.s.l. Grinding (Grinding or Milling) [Online]. Available from: http://www.thaiceramicsociety.com/pc_pre_grindmore.php [2015, January 15]

[30] Kumar, S., Drozd, V., and Saxena, S. Catalytic Studies of Sodium Hydroxide and Carbon Monoxide Reaction. Catalysts 2(4) (2012): 532-543.

[31] Mohamed, A.R., Zakaria, Z., and Zulkali, M.M.D. Catalytic Hydrogenation of Carbon Dioxide by Platinum Doped Nickel Oxide Catalysts. world Applied Sciences Journal 8 (2010): 490-495.

[32] Shin, W.G., Jung, H.J., Sung, H.G., Hyun, H.S., and Sohn, Y. Synergic CO oxidation activities of boron–CeO_2 hybrid materials prepared by dry and wet milling methods. Ceramics International 40(8) (2014): 11511-11517.

[33] Zhang, C., Li, S., Wu, G., and Gong, J. Synthesis of stable Ni-CeO2 catalysts via ball-milling for ethanol steam reforming. Catalysis Today 233 (2014): 53-60.

[34] Li, Y., Xie, W., and Yong , S. The acidity and catalytic behavior of Mg-ZSM-5 prepared via a solid-state reaction. Applied Catalysis 150 (1997): 231-242

[35] Das, T. and Deo, G. Effects of metal loading and support for supported cobalt catalyst. Catalysis Today 198(1) (2012): 116-124.

[36] Nickel Available from: https://en.wikipedia.org/wiki/Nickel [2015, January 15]

[37] Stiles, A.B. Catalyst supports and supported catalysts. 80 Montvale Avenue Stoneham. MA02180: Butterworth Publshers 1987.

[38] Kok, E., Scott, J., Cant, N., and Trimm, D. The impact of ruthenium, lanthanum and activation conditions on the methanation activity of alumina-supported cobalt catalysts. Catalysis Today 164(1) (2011): 297-301.

[39] Znak, L., Stołecki, K., and Zieliński, J. The effect of cerium, lanthanum and zirconium on nickel/alumina catalysts for the hydrogenation of carbon oxides. Catalysis Today 101(2) (2005): 65-71.

[40] Hwang, S., et al. Hydrogenation of carbon monoxide to methane over mesoporous nickel-M-alumina (M=Fe, Ni, Co, Ce, and La) xerogel catalysts. Journal of Industrial and Engineering Chemistry 18(1) (2012): 243-248.

[41] Meng, F., Zhong, P., Li, Z., Cui, X., and Zheng, H. Surface Structure and Catalytic Performance of Ni-Fe Catalyst for Low-Temperature CO Hydrogenation. Journal of Chemistry 2014 (2014): 1-7.

[42] Zhang, J., Xu, H., Jin, X., Ge, Q., and Li, W. Characterizations and activities of the nano-sized Ni/Al_2O_3 and Ni/La–Al_2O_3 catalysts for NH_3 decomposition. Applied Catalysis A: General 290(1-2) (2005): 87-96.

[43] Zhao, A., Ying, W., Zhang, H., Ma, H., and Fang, D. Ni–Al_2O_3 catalysts prepared by solution combustion method for syngas methanation. Catalysis Communications 17 (2012): 34-38.

[44] Romero, A., Jobbágy, M., Laborde, M., Baronetti, G., and Amadeo, N. Ni(II)–Mg(II)–Al(III) catalysts for hydrogen production from ethanol steam reforming: Influence of the activation treatments. Catalysis Today 149(3-4) (2010): 407-412.

[45] Didier, T., Francisco, M., Bernard, C., and Roger, D. Activation under oxidizing and reducing atmospheres of Ni-containing layered double hydroxides. Applied Catalysis A: General 159 (1997): 241-258.

[46] Zhang, Z. and Verykios, X.E. Carbon dioxide reforming of methane to synthesis gas over Ni/La_2O_3 catalysts. Applied Catalysis A: General 138 (1996): 109-133

จุฬาลงกรณ์มหาวิทยาลัย
Chulalongkorn University

[47] Iqbal, J., Wang, B., Liu, X., Yu, D., He, B., and Yu, R. Oxygen-vacancy-induced green emission and room-temperature ferromagnetism in Ni-doped ZnO nanorods. New Journal of Physics 11(6) (2009): 063009.

APPENDIX

จุฬาลงกรณ์มหาวิทยาลัย
Chulalongkorn University

APPENDIX A

CALCULATION FOR CATALYST PREPARATION

A.1 The preparation of promoted Ni/Al_2O_3 catalysts with Ce and K prepared by solid-state reaction method

Preparation of promoted Ni/Al_2O_3 catalysts by solid-state reaction between gibbsite, nickel nitrate and different promoters (potassium nitrate and cerium nitrate) are shown as followed:

Example of the calculation for the preparation of the ss_Ni-K/Al_2O_3 of the mechanical mixture of gibbsite ($Al(OH)_3$), nickel nitrate ($Ni(NO_3)_2 \cdot 6H_2O$, and potassium nitrate (KNO_3) with percent loading of 20 percent by weight of Ni and 1 percent by weight of K are shown as followed:

Reagent: Gibbsite ($Al(OH)_3$) Molecular weight = 78 g/mol

Nickel (II) nitrate hexahydrate ($Ni(NO_3)_2 \cdot 6H_2O$ Molecular weight = 290.79 g/mol

Potassium nitrate (KNO_3) Molecular weight = 101.10 g/mol

Calculation: preparing 2 g of promoted Ni/Al_2O_3 catalysts with percent loading of 20 wt% Ni and 1 wt% K are shown as followed:

100 g of promoted Ni/Al_2O_3 catalysts consisted of nickel equal to 20 g

2 g promoted Ni/Al_2O_3 catalysts consisted of nickel equal to 0.4 g

100 g promoted Ni/Al_2O_3 catalysts consisted of potassium equal to 1 g

2 g promoted Ni/Al_2O_3 catalysts consisted of potassium equal to 0.02 g

100 g promoted Ni/Al_2O_3 catalysts consisted of alumina equal to 79 g

2 g modified Ni/Al_2O_3 catalysts consisted of alumina equal to 1.58 g

The amount of nickel required 0.4 g that can be prepared from the nickel precursor was $(Ni(NO_3)_2 \cdot 6H_2O$ which had the molecular weight of 290.79 g/mol, and the molecular weight of nickel is 58.693 g/mol. Therefore, the amount of required $(Ni(NO_3)_2 \cdot 6H_2O$ can be calculated as followed:

$$(Ni(NO_3)_2.6H_2O \text{ required} = \frac{(\text{MW of } (Ni(NO_3)_2 \cdot 6H_2O) \times (\text{Nickel required})}{(\text{MW of Ni})}$$

$$= \frac{(290.79 \text{ g/mol}) \times (0.4 \text{ gNi})}{(58.693 \text{ g Ni/mol})}$$

$$= 1.9818 \text{ g of } (Ni(NO_3)_2 \cdot 6H_2O$$

The amount of potassium required 0.02 g that can be prepared from the potassium precursor was KNO_3 which had the molecular weight of 101.10 g/mol, and the molecular weight of K is 39.0983 g/mol. Therefore, the amount of required KNO_3 can be calculated as followed:

$$KNO_3 \text{ required} = \frac{(\text{MW of } KNO_3) \times (\text{K required})}{(\text{MW of K})}$$

$$= \frac{(101.10 \text{ g/mol}) \times (0.02 \text{ g K})}{(39.0983 \text{ g K /mol})}$$

$$= 0.0517158 \text{ g of } KNO_3$$

Alumina(Al_2O_3) 1.58 g consisted of aluminium (Al) equal to:

$$Al = 1.58\ g\ Al_2O_3 \times \frac{1\ mol\ Al_2O_3}{101.961\ g\ Al_2O_3} \times \frac{2\ mol\ Al}{1\ mol\ Al_2O_3} \times \frac{26.982\ g\ Al}{1\ mol\ Al}$$

$$= 0.8362\ g\ Al$$

The amount of aluminium required 0.8362 g that can be prepared from the gibbsite was ($Al(OH)_3$) which had the molecular weight of 78 g/mol, and the molecular weight of Al is 26.982 g/mol. Therefore, the amount of required ($Al(OH)_3$) can be calculated as followed:

$$(Al(OH)_3)\ required = \frac{(MW\ of\ (Al(OH)_3)) \times (Al\ required)}{(MW\ of\ Al)}$$

$$= \frac{(78\ g/mol) \times (0.8362\ g\ Al)}{(26.982\ g\ Al/mol)}$$

$$= 2.4174\ g\ of\ (Al(OH)_3)$$

In the same method preparing of promoted Ni/Al_2O_3 catalysts uses the same calculation which can use the other of promoter such as cerium nitrate.

A.2 Preparation of promoted Ni/Al_2O_3 catalysts with Ce, K, La, Mg and Mn by incipient wetness impregnation

Preparation of promoted Ni/Al_2O_3 catalysts by incipient wetness impregnation between gibbsite, nickel nitrate and different promoters (cerium nitrate, potassium nitrate, lanthanum nitrate, magnesium nitrate, manganese acetate) are shown as followed:

Example calculation for the preparation of the imp_Ni-K/Al_2O_3 of the mixing of nickel nitrate ($Ni(NO_3)_2 \cdot 6H_2O$, and potassium nitrate (KNO_3) aqueous solutions on gamma alumina (γ-Al_2O_3), percent loading of 20 percent by weight of Ni and 1 percent by weight of K are shown as followed:

Calculation: For percent loading of 20 wt% Ni and 1 wt% K are shown as follows:

Based on 2 g of promoted Ni/Al_2O_3 catalysts:

100 g promoted Ni/Al_2O_3 catalysts consisted of nickel equal to 20 g Ni

2 g promoted Ni/Al_2O_3 catalysts consisted of nickel equal to 0.4 g Ni

100 g promoted Ni/Al_2O_3 catalysts consisted of potassium equal to 1 gK

2 g promoted Ni/Al_2O_3 catalysts consisted of manganese equal to 0.02 gK

100 g modified Ni/Al_2O_3 catalysts consisted of alumina equal to 79 g Al_2O_3

2 g modified Ni/Al_2O_3 catalysts consisted of alumina equal to 1.58 g Al_2O_3

The amount of nickel required 0.4 g that can be prepared from the nickel precursor was $Ni(NO_3)_2 \cdot 6H_2O$ which had the molecular weight of 290.79 g/mol, and

the molecular weight of nickel is 58.693 g/mol. Therefore, the amount of required $(Ni(NO_3)_2 \cdot 6H_2O$ can be calculated as followed:

$$(Ni(NO_3)_2.6H_2O \text{ required} = \frac{(\text{MW of } (Ni(NO_3)_2 \cdot 6H_2O) \times (\text{Nickel required})}{(\text{MW of Ni})}$$

$$= \frac{(290.79 \text{ g/mol}) \times (0.4 \text{ gNi})}{(58.693 \text{ g Ni/mol})}$$

$$= 1.9818 \text{ g of } (Ni(NO_3)_2 \cdot 6H_2O$$

The amount of potassium required 0.02 g that can be prepared from the potassium precursor was KNO_3 which had the molecular weight of 101.10 g/mol, and the molecular weight of K is 39.0983 g/mol. Therefore, the amount of required KNO_3 can be calculated as followed:

$$KNO_3 \text{ required} = \frac{(\text{MW of } KNO_3) \times (\text{K required})}{(\text{MW of K})}$$

จุฬาลงกรณ์มหาวิทยาลัย
Chulalongkorn University

$$= \frac{(101.10 \text{ g/mol}) \times (0.02 \text{ g K})}{(39.0983 \text{ g K /mol})}$$

$$= 0.0517158 \text{ g of } KNO_3$$

For Alumina(Al_2O_3), the amount of 1.58 g are required for preparing 2 g of promoted Ni/Al_2O_3 catalysts.

In the same method preparing of promoted Ni/Al_2O_3 catalysts uses the same calculation which can use the other of promoter such as cerium nitrate.

APPENDIX B

CALCULATION OF THE CRYSTALLITE SIZE

Calculation of the crystallite size by Scherrer equation

The average crystallite sizes of NiO were calculated by the Scherrer's equation using the full width at half maximum of the diffraction peak of XRD

From Scherrer equation:

$$D = \frac{K\lambda}{\beta \cos\theta}$$

Where D = Crystallite size, Å

K = Crystallite-shape factor = 0.9

λ = X-ray wavelength, 1.54056 Å for CuK_{α}

θ = Observed peak angle, degree

β = X-ray diffraction broadening, radian

The X-ray diffraction broadening (β) is the pure width of powder diffraction free of all broadening due to the experiment equipment. Standard α-alumina is used to observe the instrumental broadening since its crystallite size is larger than 2000 Å. The X-ray diffraction broadening (β) can be obtained by using Warren's formula

From Warren's formula:

$$\beta_2 = \beta_{2M} - \beta_{2S}$$

$$\beta = \sqrt{\beta_M^{\,2} - \beta_S^2}$$

Where β_M = The measured peak width in radians at half peak height

β_S = The corresponding width of a standard material

Example: Calculation of the NiO crystallite size on Al_2O_3 support of imp_Ni-Ce/Al_2O_3

The half-height width of peak = 0.6105° (from Figure B.1)

= 0.6105 × 0.0174

= 0.01065 radian

The corresponding half-height width of peak of α-alumina = **0.**000787 radian

The pure width $\beta = \sqrt{\beta_M^{\,2} - \beta_S^2}$

$= \sqrt{0.01065^{\,2} - 0.000787^{\,2}}$

= 0.01062

จุฬาลงกรณ์มหาวิทยาลัย
Chulalongkorn University

β = 0.01062 radian

2θ = 43.48°

θ = 21.74° = 0.3793 radian

λ = 1.54056 Å

$$\text{The crystallite size} = \frac{0.9 \times 1.54056}{(0.1062)\cos 0.3793}$$

= 140.53 Å

= 14.1 nm

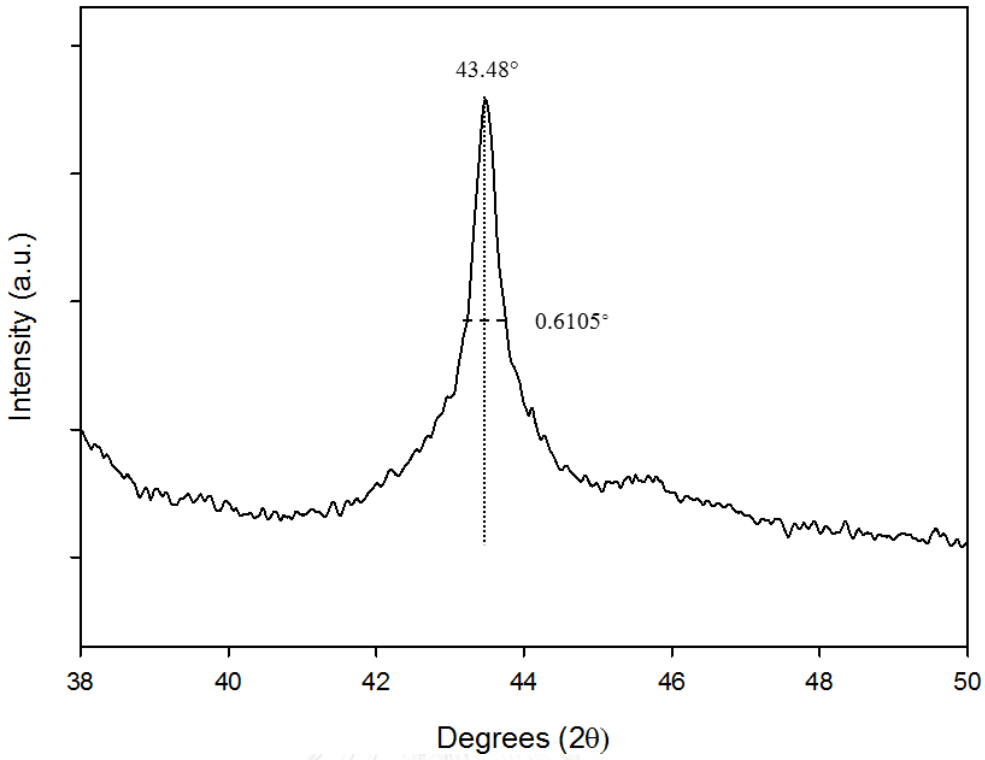

Figure B.1 The measured peak of imp_Ni-K/Al_2O_3 to calculate the crystallite size

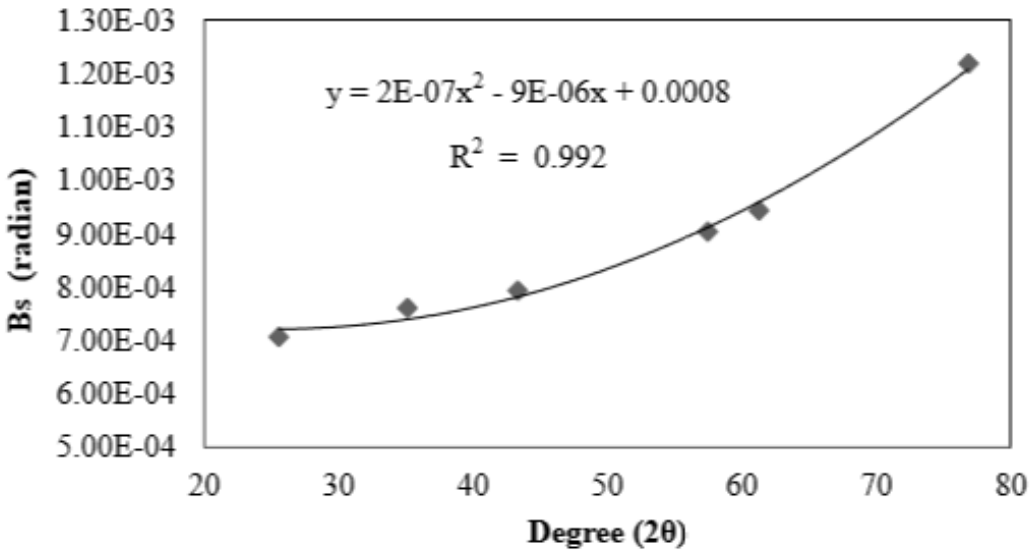

Figure B.2 The plot indicating the value of line broadening due to the equipment that was obtained by using **α**-alumina as standard.

APPENDIX C

CALCULATION FOR TOTAL CO CHEMISORPTION

Calculation of the amount of Ni active sites and the % dispersion, which a stoichiometry of CO/Ni = 1(S_f=1), measured by CO chemisorption is as follows:

The weight of catalyst used	=	W	g
Loop volume dosed	=	V_{loop}	µL
Integral area of CO peak after adsorption	=	A_i	unit
Integral area of 20 µL of standard CO peak	=	A_f	unit
Molar volume of gas at STP (V_g)	=	22414	cm^3/mol
% Metal used	=	%M	%
Molecular weight of the metal	=	MW.	a.m.u.
Avogadro's number	=	6.023×10^{23}	molecules/mol
Stoichiometry factor	=	S_f	

Amount of CO adsorbed on catalyst $= \dfrac{V_{loop} \times \sum (A_f - A_i)}{(W - A_f)} = A$ µL/gcat

Amount of CO adsorbed on catalyst (V_{ads}) = A/1000 = B cm^3/gcat

Molecule of CO adsorbed on catalyst = Metal active site

$$= S_f \times \frac{V_{ads}}{V_g} \times 6.023 \times 10^{23} \text{ molecules/g.cat}$$

%Dispersion

$$= S_f \times \frac{V_{ads}}{V_g} \times \frac{m.w.}{\%M} \times 100\% \times 100\%$$

APPENDIX D

CALIBRATION CURVES

For appendix D, presenting the calibration curves, is used for calculation of the composition in CO_2 hydrogenation reaction, which are, carbon dioxide as reactant and methane as main product, including carbon monoxide is a by-product.

Shimadzu GC-8A (molecular sieve 5Å column) gas chromatograph equipped with Thermal conductivity detector (TCD).

In presented calibrations curves of CO_2, CO, and CH_4, the x-axis displayed the area and the y-axis displayed the mole of reagent which reported by gas chromatography.

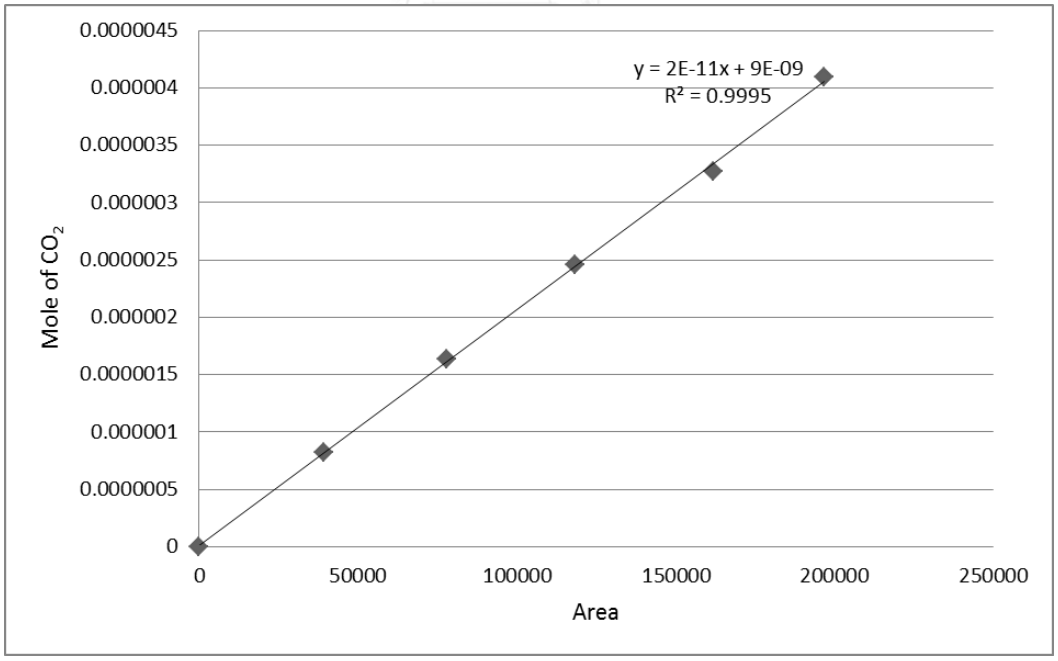

Figure D.1 The calibration curve of carbon dioxide

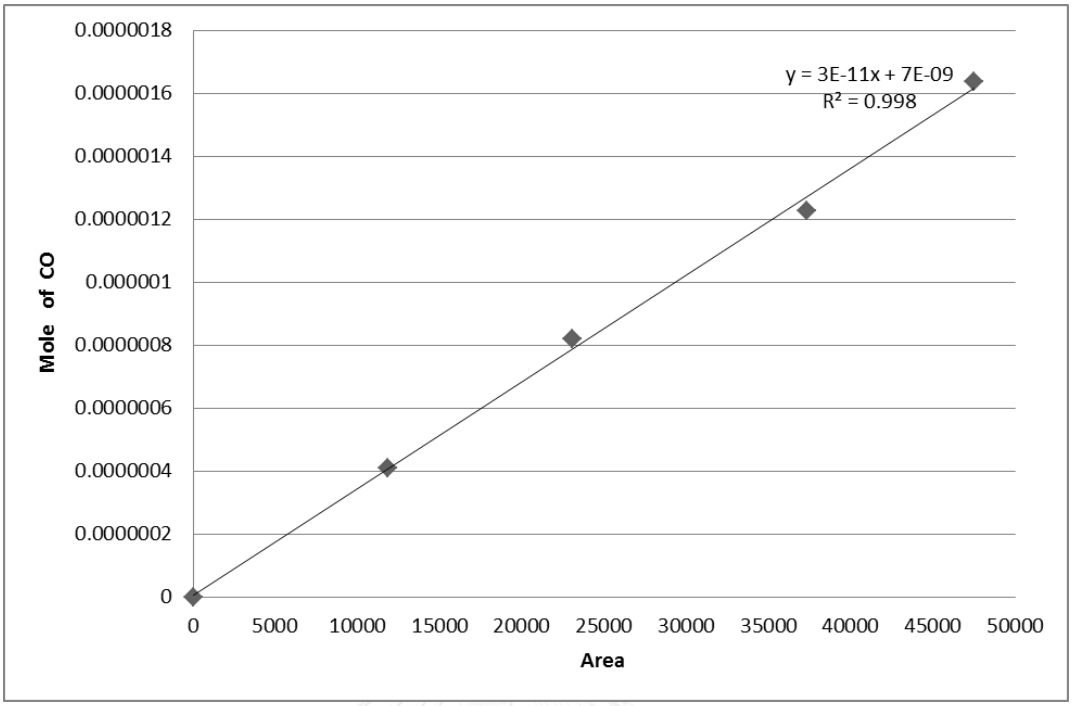

Figure D.2 The calibration curve of carbon monoxide

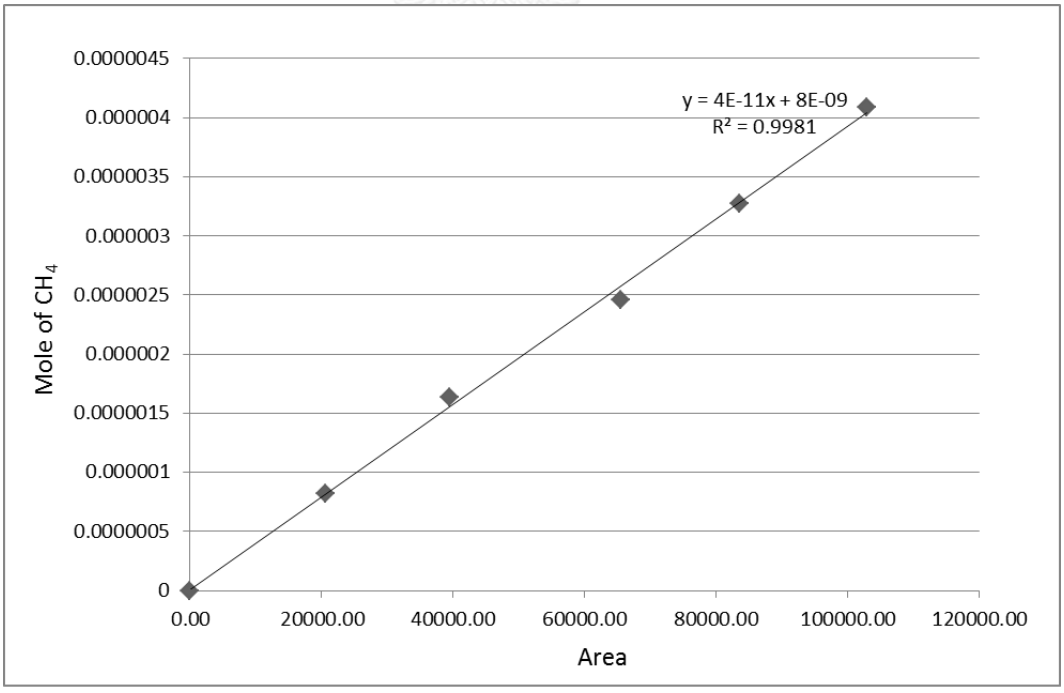

Figure D.3 The calibration curve of methane

Table D.1 Condition use in Shimadzu modal GC-8A

Parameters	Condition Shimadzu GC-8A (TCD)
Width	5
Slope	50
Drift	0
Min. area	10
T.DBL	0
Stop time	12
Atten	5
Speed	10
Method	1
Format	1
SPL.WT	100
IS.WT	1

จุฬาลงกรณ์มหาวิทยาลัย
Chulalongkorn University

VITA

Miss Phirunlak Boonyawat was born on 2nd May 1991, in Bangkok, Thailand. She graduated in Bachelor degree from faculty of science in Chemical Technology, Chulalongkorn University, Thailand in April 2013. Since 29 April 2013. She has been studying in Master degree of Chemical Engineering from faculty of Engineer, Chulalongkorn University.

List of publication:

Phirunlak Boonyawat, and Joongjai Panpranot, “The effect of promoters on nickel/alumina catalysts in the hydrogenation of CO2”, Proceedings of The 4th TIChE International Conference 2014 and The 24th Thai Institute of Chemical Engineering and Applied Chemistry Conference in Chiang Mai, Thailand, December 18-19, 2014.

จุฬาลงกรณ์มหาวิทยาลัย
Chulalongkorn University